

# From topological amplitude to rescattering dynamics

Di Wang<sup>1\*</sup>

<sup>1</sup>*Department of Physics, Hunan Normal University,  
and Key Laboratory of Low-Dimensional Quantum Structures and  
Quantum Control of Ministry of Education, Changsha 410081, China*

## Abstract

We proposed a theoretical framework to correlate the topological diagram at quark level and rescattering dynamics at hadron level. In the framework, both the hadronic triangle diagram, and the quark diagram, which is the intermediate structure between topological diagram and triangle diagram, are expressed in the tensor form. The completeness of quark diagram is confirmed by the quark substructure of meson-meson scattering. The coefficient of each triangle diagram can be derived from the quark diagram and the total rescattering amplitudes are consistent with the ones derived from the chiral Lagrangian. If only the short-distance  $T$  diagram is considered as the weak vertex in triangle diagram, the rescattering contributions in the  $C$ ,  $E$  and  $P$  diagrams have definite proportional relation of  $L(C) : L(E) : L(P) = -2 : 1 : 1$  under the  $SU(3)_F$  symmetry, and the rescattering contributions in the  $T$  and  $A$  diagrams are only arisen from the  $SU(3)_F$  breaking effects. Taking  $D \rightarrow K\pi$  and  $D \rightarrow \pi\pi$  decays as examples, we present our framework in detail. We find the Isospin relations in these decays are still valid in terms of triangle diagrams. Besides, the conclusions in the  $D$  meson decays under the  $SU(3)_F$  symmetry can be generalized to the  $B$  meson decays under the  $SU(4)_F$  symmetry.

---

\*Electronic address: wangdi@hunnu.edu.cn

## I. INTRODUCTION

Heavy meson/baryon non-leptonic decay provides an ideal platform to test the Standard Model (SM) and search for new physics. Many data have been collected by experiments in the last few decades [1]. The non-perturbative QCD dynamics is still a challenge in theory, especially in charmed hadron decay. The QCD-inspired approaches, such as QCD factorization (QCDF) [2–5], perturbative QCD approach (PQCD) [6–9], and soft-collinear effective theory (SCET) [10, 11], do not work well in charm sector because of the large expansion parameters  $\alpha_s(m_c)$  and  $\Lambda_{\text{QCD}}/m_c$ . An alternative way to investigate the charmed hadron decay is the flavor symmetry analysis. The topological diagram amplitude (TDA) approach [12–16], in which the topological diagrams are classified according to the topologies in the flavor flow of weak decay diagrams, is very popular. Topological diagram is intuitive to the internal dynamics of hadron decays, providing a framework in which we cannot only do a model-dependent data analysis [17–22] but also perform a theoretical model calculation [23–31]. In Refs. [32–34], a systematic method to treat the topological amplitudes was proposed. In the framework, the topologies are expressed in invariant tensors and the universality, completeness and correlation of topology are clarified.

Another approach to study the non-perturbative QCD effects is the rescattering mechanism. In this framework, the non-perturbative QCD effects are modeled as an exchange of one particle between two particles generated from the short-distance tree emitted process. It forms a triangle diagram at hadron level. The rescattering mechanism was used to estimate the branching fractions of heavy meson and baryon hadron decays [35–44]. In 2017, the rescattering mechanism was extended to the doubly charmed baryon decays, helping us observe  $\Xi_{cc}^{++}$  for the first time [45, 46]. After that, the branching fractions of other doubly charmed baryon decay channels were estimated in the rescattering mechanism [47, 48].

The topological amplitude and rescattering dynamics seems to be two unrelated theories since one is at the quark level and the other is at the hadron level. In Refs. [38–40], the authors attempted to establish the relation between the topological diagram and triangle diagram via the intermediate structure between them, quark diagram. Because of the absence of a systematic method, they did not find all the quark diagrams, resulting in some confusions. For example, the Isospin factor  $1/\sqrt{2}$  or  $-1/\sqrt{2}$  is added manually in Ref. [38] to satisfy Isospin relation of the  $D^+ \rightarrow \pi^+\pi^0$ ,  $D^0 \rightarrow \pi^+\pi^-$  and  $D^0 \rightarrow \pi^0\pi^0$  modes without a convictive argument. And the triangle diagrams extracted by quark diagrams are in conflict with the ones derived from the chiral Lagrangian [40]. Thereby, a systematic study of the relation between the topological amplitude and the rescattering dynamics

is necessary.

Inspired by Refs. [32–34], we find that the quark diagram can also be expressed in tensor form just like topological diagram. Meanwhile, the quark diagram written in tensor form can be understood as triangle diagrams in the rescattering dynamics. As a result, the algebraic tensor serves as a bridge between the topological diagram at quark level and the triangle diagram in hadron level. The completeness of the quark diagram is confirmed by the quark substructure of meson-meson scattering. The coefficient of each triangle diagram, such as Isospin factor, can be derived from the quark diagram. The triangle diagrams derived from the topological diagrams are consistent with the ones derived from the chiral Lagrangian.

Taking  $D \rightarrow K\pi$  and  $D \rightarrow \pi\pi$  decays as examples, we present our framework in detail. We find the triangle diagrams with vertexes of  $\omega\pi\pi$ ,  $\rho^0\pi^0\pi^0 \dots$  cancel each other after summing all triangle diagrams in one decay channel. The Isospin relations hold in terms of the triangle diagrams. Under the  $SU(3)_F$  symmetry, the rescattering contributions arisen from  $T^{SD}$  in the  $C$ ,  $E$  and  $P$  diagrams have the relation of  $L(C) : L(E) : L(P) = -2 : 1 : 1$ . If the  $SU(3)_F$  symmetry breaks into the Isospin symmetry, the proportional relation is broken. The rescattering contributions arisen from  $T^{SD}$  in the  $T$  and  $A$  diagrams are only arisen from the  $SU(3)_F$  breaking effects. And there are no triangle diagram like long-distance contributions in the topologies  $ES$ ,  $AS$ ,  $PS$ ,  $PA$  and  $SS$ .

This paper is organized as follows. In Sec. II, we construct the tensor representation of quark diagram and triangle diagram, and investigate the relation between topological amplitude and rescattering dynamics. Taking  $D \rightarrow K\pi$  and  $D \rightarrow \pi\pi$  decays as examples, we show the reliability of our method and give some conclusions in Sec. III. Sec. IV is a short summary. Further discussions in the  $\bar{B} \rightarrow D\pi$  and  $\bar{B} \rightarrow \pi\pi$  decays can be found in Appendix. A.

## II. FROM TOPOLOGICAL DIAGRAM TO TRIANGLE DIAGRAM

In this section, we first review the basic idea of the topological diagram expressed in the invariant tensor, taking the  $D \rightarrow PP$  decay as examples. Then we try to write the quark diagram and triangle diagram in the tensor form and analyze the relation among topological diagram, quark diagram and triangle diagram.

In the  $SU(3)$  picture, the pseudoscalar meson notet  $|P_j^i\rangle$  is expressed as

$$|P_j^i\rangle = \begin{pmatrix} \frac{1}{\sqrt{2}}|\pi^0\rangle + \frac{1}{\sqrt{6}}|\eta_8\rangle, & |\pi^+\rangle, & |K^+\rangle \\ |\pi^-\rangle, & -\frac{1}{\sqrt{2}}|\pi^0\rangle + \frac{1}{\sqrt{6}}|\eta_8\rangle, & |K^0\rangle \\ |K^-\rangle, & |\bar{K}^0\rangle, & -\sqrt{\frac{2}{3}}|\eta_8\rangle \end{pmatrix} + \frac{1}{\sqrt{3}} \begin{pmatrix} |\eta_1\rangle, & 0, & 0 \\ 0, & |\eta_1\rangle, & 0 \\ 0, & 0, & |\eta_1\rangle \end{pmatrix}, \quad (1)$$

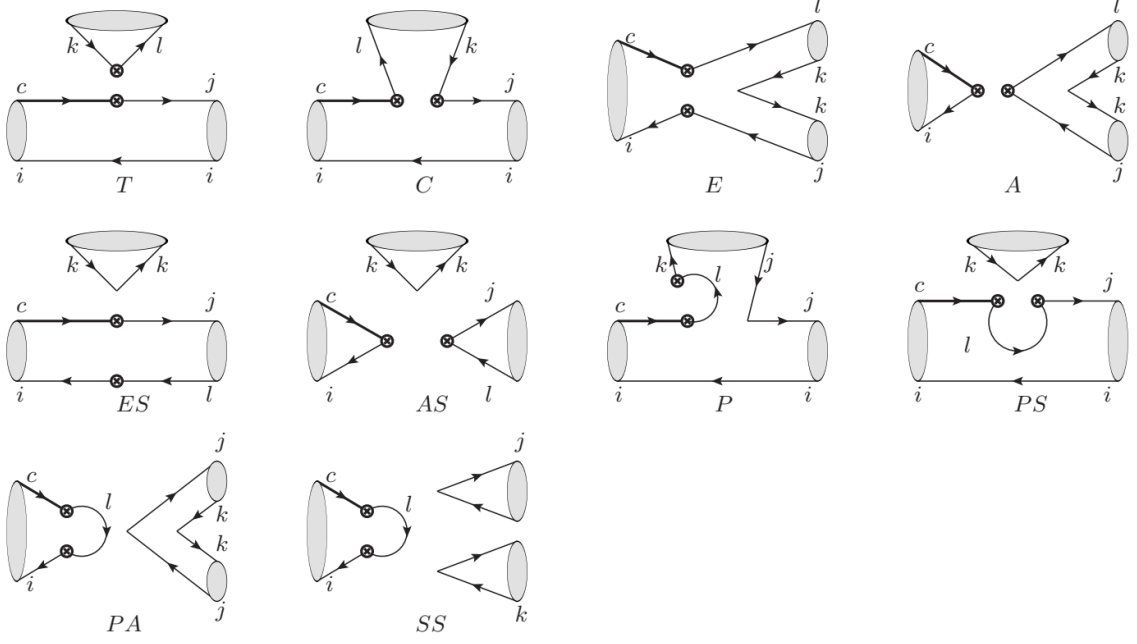


FIG. 1: Topological diagrams contributing to the  $D \rightarrow PP$  decay in the Standard Model.

where  $i$  is row index and  $j$  is column index. The vector meson nonet is

$$|V\rangle_j^i = \begin{pmatrix} \frac{1}{\sqrt{2}}|\rho^0\rangle + \frac{1}{\sqrt{2}}|\omega\rangle, & |\rho^+\rangle, & |K^{*+}\rangle \\ |\rho^-\rangle, & -\frac{1}{\sqrt{2}}|\rho^0\rangle + \frac{1}{\sqrt{2}}|\omega\rangle, & |K^{*0}\rangle \\ |K^{*-}\rangle, & |\bar{K}^{*0}\rangle, & |\phi\rangle \end{pmatrix}. \quad (2)$$

The charmed meson anti-triplet state is

$$|D^i\rangle = (|D^0\rangle, |D^+\rangle, |D_s^+\rangle). \quad (3)$$

The topological amplitude of the  $D \rightarrow PP$  decay in the SM can be written as

$$\begin{aligned} \mathcal{A}(D \rightarrow PP) = & T \cdot D_i H_k^{lj} P_j^i P_l^k + C \cdot D_i H_k^{jl} P_j^i P_l^k + E \cdot D_i H_j^{il} P_k^j P_l^k + A \cdot D_i H_j^{li} P_k^j P_l^k \\ & + ES \cdot D_i H_l^{ij} P_j^l P_k^k + AS \cdot D_i H_l^{ji} P_j^l P_k^k + P \cdot D_i H_l^{kl} P_j^i P_k^j + PS \cdot D_i H_l^{jl} P_j^i P_k^k \\ & + PA \cdot D_i H_l^{il} P_k^j P_j^k + SS \cdot D_i H_l^{il} P_j^j P_k^k. \end{aligned} \quad (4)$$

If the index-contraction is understood as quark flowing, each term in Eq. (4) is a topological diagram, see Fig. 1. The first four diagrams,  $T$ ,  $C$ ,  $E$  and  $A$ , have been analyzed in plenty of literature.  $ES$  and  $AS$  are the singlet contributions which require multi-gluon exchanges. The last four diagrams are quark-loop contributions. More details about topological amplitudes can be found in Ref. [34].

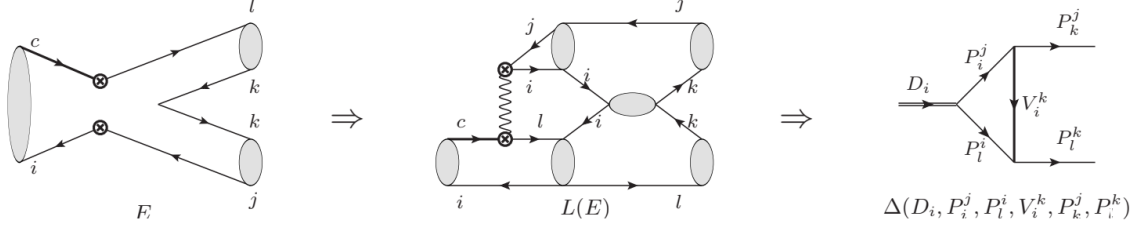


FIG. 2: Topological diagram  $\Rightarrow$  Quark diagram  $\Rightarrow$  Triangle diagram in  $T \Rightarrow E$  transition.

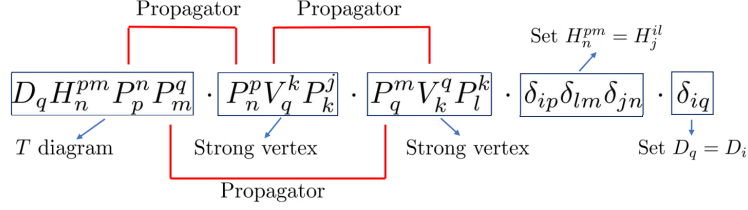


FIG. 3: The triangle diagram constructed by the quark diagram in  $T \Rightarrow E$  transition.

Next, we express the quark diagram and triangle diagram in the tensor form, taking  $E$  diagram as an example. The rescattering contribution in  $E$  diagram can be obtained by twisting quark lines from a short-distance  $T$  diagram. We call it " $T \Rightarrow E$ " transition. The superscripts "SD" and "LD" are dropped for convenience. The intermediate structure of  $T \Rightarrow E$  transition is called quark diagram  $L(E)$ . And the quark diagram  $L(E)$  forms a triangle diagram at hadron level, see Fig. 2. In the tensor form of topological diagram,  $T$  diagram is written as  $D_q H_n^{pm} P_p^n P_m^q$ , and  $E$  diagram is written as  $D_i H_j^{il} P_k^j P_l^k$ . Then the quark diagram of  $T \Rightarrow E$  transition can be written as

$$L(E)[i, j, k, l] = D_q H_n^{pm} P_p^n P_m^q \cdot P_n^p V_q^k P_k^j \cdot P_q^m V_k^q P_l^k \cdot \delta_{ip} \delta_{lm} \delta_{jn} \cdot \delta_{iq}. \quad (5)$$

$L(E)[i, j, k, l]$  can also be understood as a triangle diagram, see Fig. 3. The  $T$  diagram in the left is the weak vertex of  $D_q \rightarrow P_p^n P_m^q$  in the triangle diagram. The two  $PVP$  vertexes are two strong vertexes. The index contractions of  $P_p^n P_m^q$ ,  $P_n^p P_m^q$  and  $V_q^k V_k^q$  are three meson propagators. The kronecker symbols are used to set  $H_n^{pm} = H_j^{il}$  and  $D_q = D_i$ . Notice that we only consider the vector meson exchange here, i.e.,  $D \rightarrow PP \rightarrow PP$  via exchanging a vector meson. For the processes such as  $D \rightarrow VV \rightarrow PP$  via exchanging a pseudoscalar meson, the analysis is the similar to the case of  $D \rightarrow PP \rightarrow PP$ . We shall not discuss it in this work.

Similar to the  $E$  diagram, the quark diagram in  $T \Rightarrow C$  transition can be written as

$$L(C)_1[i, j, k, l] = D_q H_n^{pm} P_p^n P_m^q \cdot P_n^p V_i^n P_j^i \cdot P_q^m V_k^q P_l^k \cdot \delta_{jp} \delta_{lm} \delta_{kn} \cdot \delta_{iq}, \quad (6)$$

$$L(C)_2[i, j, k, l] = D_q H_n^{pm} P_p^n P_m^q \cdot P_n^p V_p^l P_l^k \cdot P_q^m V_m^j P_j^i \cdot \delta_{jp} \delta_{lm} \delta_{kn} \cdot \delta_{iq}. \quad (7)$$

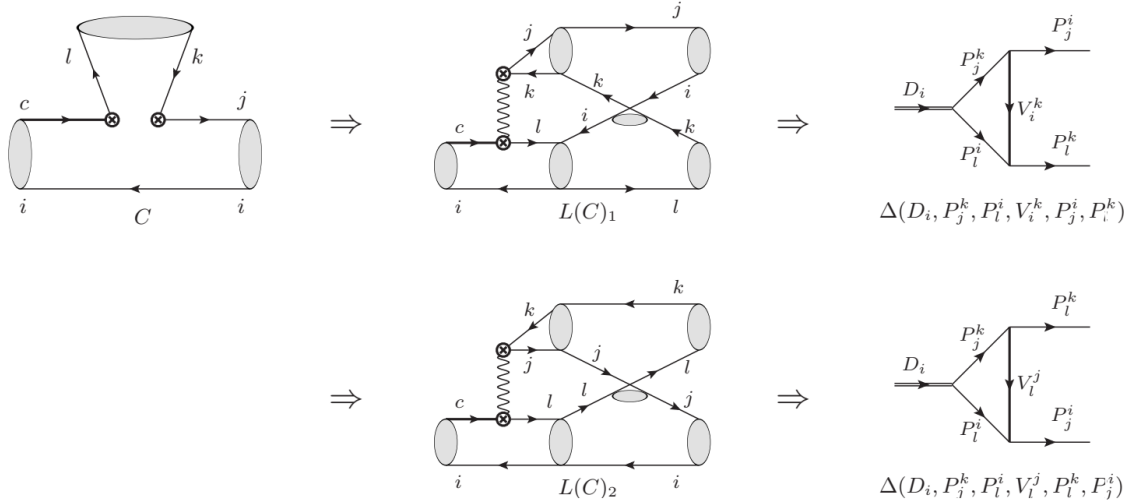


FIG. 4: Topological diagram  $\Rightarrow$  Quark diagram  $\Rightarrow$  Triangle diagram in  $T \Rightarrow C$  transition.

The diagrams are presented in Fig. 4. Compared to the quark diagram  $L(E)$ , the two quark diagrams  $L(C)_1$  and  $L(C)_2$  have a cross in the above strong vertex. This cross will contribute a minus sign in the triangle diagrams because of the commutator in chiral Lagrangian. To make it clear, we analyze the strong vertexes of  $\rho^0 \rightarrow \pi^+\pi^-$  and  $\omega \rightarrow \pi^+\pi^-$ . The chiral Lagrangian of  $V \rightarrow PP$  decay is

$$\mathcal{L}_{VPP} = \frac{i}{\sqrt{2}} g_{VPP} \text{Tr}[V^\mu [P, \partial_\mu P]]. \quad (8)$$

Inserting the pseudoscalar meson notet and vector meson nonet, one can get the strong vertexes of  $\rho^0 \rightarrow \pi^+\pi^-$  and  $\omega \rightarrow \pi^+\pi^-$  are

$$\begin{aligned} \mathcal{L}_{VPP} = & \frac{i}{\sqrt{2}} g_{VPP} [\dots + (\frac{1}{\sqrt{2}} \rho^0 + \frac{1}{\sqrt{2}} \omega) [\pi^+ \partial_\mu \pi^- - \pi^- \partial_\mu \pi^+] + \dots \\ & + (-\frac{1}{\sqrt{2}} \rho^0 + \frac{1}{\sqrt{2}} \omega) [\pi^- \partial_\mu \pi^+ - \pi^+ \partial_\mu \pi^-] + \dots], \end{aligned} \quad (9)$$

in which the first line is the contributions from  $u\bar{u}$  constituent of  $\rho^0/\omega$  and the second line is the contributions from  $d\bar{d}$  constituent. The  $\omega\pi\pi$  vertexes from  $u\bar{u}$  and  $d\bar{d}$  cancel each other in the final chiral Lagrangian. At the quark level, this cancelation can be described by Fig. 5. The first diagram in Fig. 5 is the  $u\bar{u}$  contribution and the second diagram is the  $d\bar{d}$  contribution. The second diagram can be seen as an interchange of  $\pi^+$  and  $\pi^-$  in the first diagram. Because of the commutator in chiral Lagrangian, the second diagram is opposite to the second diagram. That is why  $\omega \nrightarrow \pi^+\pi^-$ . For  $\rho^0 \rightarrow \pi^+\pi^-$  decay, there is a additional minus sign in the second diagram due to Eq. (2) to get a non-zero amplitude.

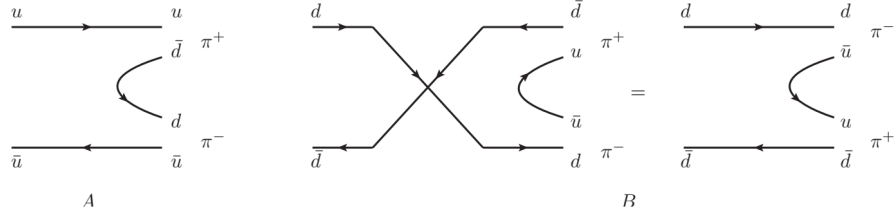


FIG. 5: Strong vertexes of  $\rho^0 \rightarrow \pi^+\pi^-$  and  $\omega \rightarrow \pi^+\pi^-$ .

The long-distance contributions in  $T$  diagram can also be modeled as meson-meson scattering between two mesons emitted from short-distance  $T$  diagram. Similar to the  $E$  and  $C$  diagrams, the quark diagram in  $T \Rightarrow T$  transition can be written as

$$L(T)_1[i, j, k, l] = D_q H_n^{pm} P_p^n P_m^q \cdot P_n^p V_k^n P_l^k \cdot P_q^m V_i^q P_j^i \cdot \delta_{lp} \delta_{jm} \delta_{kn} \cdot \delta_{iq}, \quad (10)$$

$$L(T)_2[i, j, k, l] = D_q H_n^{pm} P_p^n P_m^q \cdot P_n^p V_p^l P_l^k \cdot P_q^m V_i^q P_j^i \cdot \delta_{lp} \delta_{jm} \delta_{kn} \cdot \delta_{iq}, \quad (11)$$

$$L(T)_3[i, j, k, l] = D_q H_n^{pm} P_p^n P_m^q \cdot P_n^p V_k^n P_l^k \cdot P_q^m V_m^j P_j^i \cdot \delta_{lp} \delta_{jm} \delta_{kn} \cdot \delta_{iq}, \quad (12)$$

$$L(T)_4[i, j, k, l] = D_q H_n^{pm} P_p^n P_m^q \cdot P_n^p V_p^l P_l^k \cdot P_q^m V_m^j P_j^i \cdot \delta_{lp} \delta_{jm} \delta_{kn} \cdot \delta_{iq}. \quad (13)$$

The diagrams are presented in Fig. 6. The vector propagators in the Eqs. (10)~(13) are constructed by two dyadic tensors [49] rather than an invariant tensor such as  $V_i^k V_k^i$  in  $T \Rightarrow E$  transition. For example, the vector propagator in  $L(T)_1$  is expressed as  $V_k^n V_i^q$ . Considering  $i = q$  and  $k = n$ , it becomes  $V_k^k V_i^i$ . The upper and lower indices in  $V_k^k$  and  $V_i^i$  do not contract each other like a singlet.  $V_k^k V_i^i$  can be seen as a neutral vector propagator, such as  $\rho^0$ ,  $\omega$  ... etc. In order to clarify the difference between dyadic tensor and invariant tensor, we show the invariant tensor ( $\alpha$ ) and dyadic tensor ( $\beta$  and  $\gamma$ ) in Fig. 7. In  $\alpha$  diagram, there are two quark lines,  $\bar{i}$  and  $k$ . In  $\beta$  diagram of Fig. 7, there are four quark lines,  $i$ ,  $\bar{i}$ ,  $k$ ,  $\bar{k}$ . If  $i = k$ , we can interchange the position of  $i$  and  $k$  to transform  $\beta$  diagram to  $\gamma$  diagram. According to the Pauli exclusion principle, interchanging two fermions produces a minus sign, thus  $\beta + \gamma = 0$ . So  $\beta$  diagram is a neutral vector propagator only in the case of  $i \neq k$ .

For the completeness of our theoretical framework, we list all the tensor structures in  $T \Rightarrow A, ES, AS, P, PS, PA, SS$  transitions.

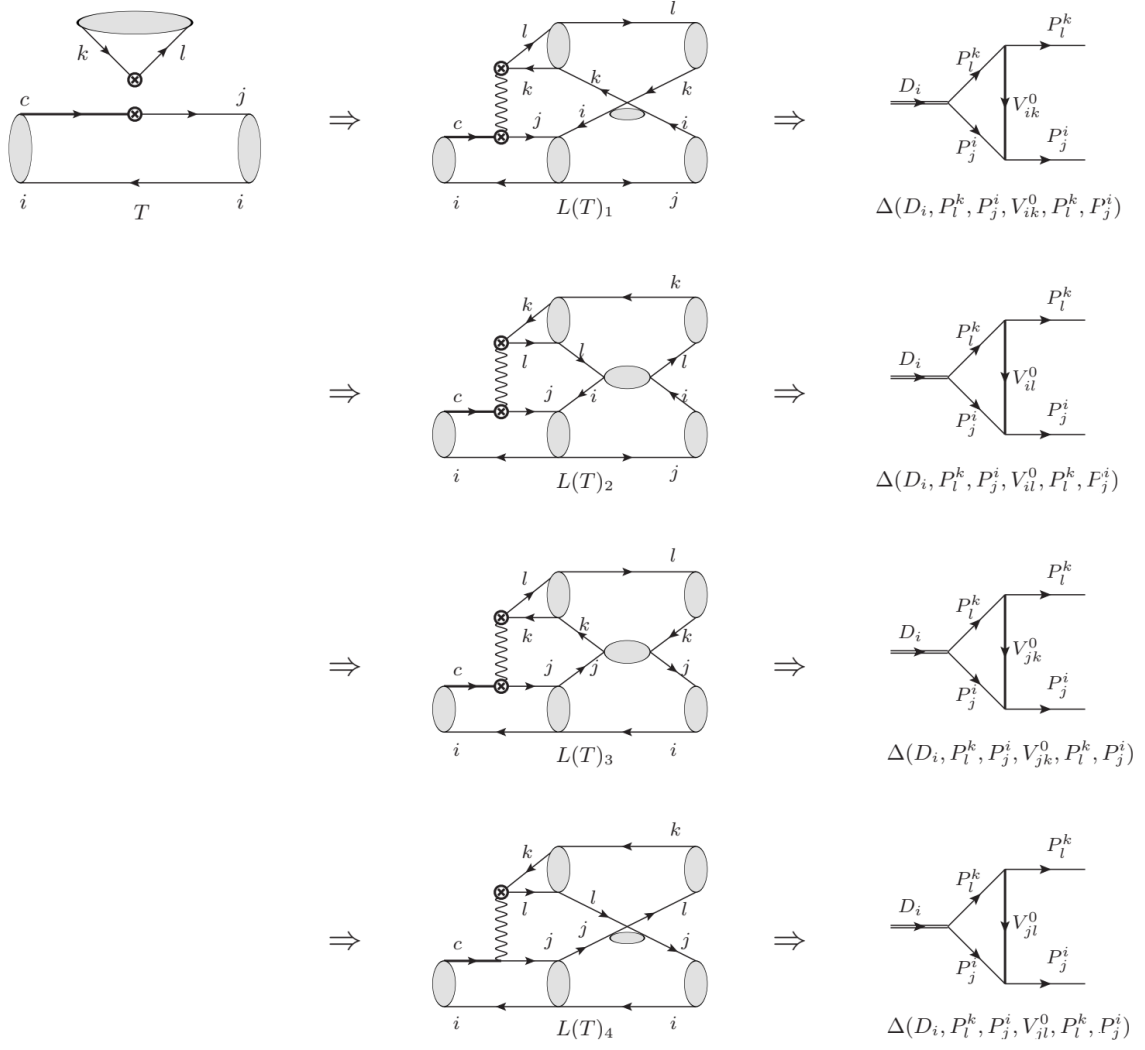


FIG. 6: Topological diagram  $\Rightarrow$  Quark diagram  $\Rightarrow$  Triangle diagram in  $T \Rightarrow T$  transition.

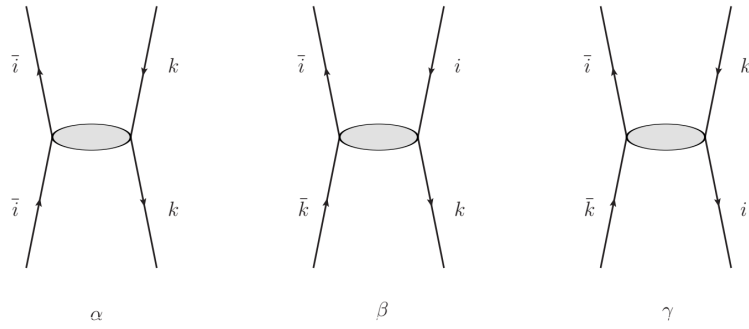


FIG. 7: Comparison between the meson propagator constructed by an invariant tensor ( $\alpha$ ) and two dyadic tensors ( $\beta$  and  $\gamma$ ).



$T \Rightarrow A$ :

$$L(A)_1[i, j, k, l] = D_q H_n^{pm} P_p^n P_m^q \cdot P_n^p V_p^k P_k^j \cdot P_k^r V_r^l P_l^k \cdot \delta_{lp} \delta_{im} \delta_{jn} \cdot \delta_{iq} \cdot \delta_{kr}, \quad (14)$$

$$L(A)_2[i, j, k, l] = D_q H_n^{pm} P_p^n P_m^q \cdot P_n^p V_k^n P_l^k \cdot P_r^k V_j^r P_k^j \cdot \delta_{lp} \delta_{im} \delta_{jn} \cdot \delta_{iq} \cdot \delta_{kr}, \quad (15)$$

$$L(A)_3[i, j, k, l] = D_q H_n^{pm} P_p^n P_m^q \cdot P_n^p V_p^k P_k^j \cdot P_r^l V_k^r P_l^k \cdot \delta_{lp} \delta_{im} \delta_{jn} \cdot \delta_{iq} \cdot \delta_{lr}, \quad (16)$$

$$L(A)_4[i, j, k, l] = D_q H_n^{pm} P_p^n P_m^q \cdot P_n^p V_k^n P_l^k \cdot P_j^r V_r^k P_k^j \cdot \delta_{lp} \delta_{im} \delta_{jn} \cdot \delta_{iq} \cdot \delta_{jr}, \quad (17)$$

$$L(A)_5[i, j, k, l] = D_q H_n^{pm} P_p^n P_m^q \cdot P_n^p V_p^k P_j^i \cdot P_q^m V_k^l P_l^k \cdot \delta_{lp} \delta_{im} \delta_{jn} \cdot \delta_{iq}, \quad (18)$$

$$L(A)_6[i, j, k, l] = D_q H_n^{pm} P_p^n P_m^q \cdot P_n^p V_k^n P_l^k \cdot P_q^m V_j^k P_k^j \cdot \delta_{lp} \delta_{im} \delta_{jn} \cdot \delta_{iq}. \quad (19)$$

$T \Rightarrow ES$ :

$$L(ES)_1[i, j, k, l] = D_q H_n^{pm} P_p^n P_m^q \cdot P_n^p V_p^j P_j^l \cdot P_q^m V_m^q P_k^k \cdot \delta_{ip} \delta_{jm} \delta_{ln} \cdot \delta_{iq}, \quad (20)$$

$$L(ES)_2[i, j, k, l] = D_q H_n^{pm} P_p^n P_m^q \cdot P_n^p V_p^n P_k^k \cdot P_q^m V_l^q P_j^l \cdot \delta_{ip} \delta_{jm} \delta_{ln} \cdot \delta_{iq}. \quad (21)$$

$T \Rightarrow AS$ :

$$L(AS)_1[i, j, k, l] = D_q H_n^{pm} P_p^n P_m^q \cdot P_n^p V_l^n P_j^l \cdot P_r^s V_s^k P_k^r \cdot \delta_{jp} \delta_{im} \delta_{ln} \cdot \delta_{iq} \cdot \delta_{kr} \cdot \delta_{ks}, \quad (22)$$

$$L(AS)_2[i, j, k, l] = D_q H_n^{pm} P_p^n P_m^q \cdot P_n^p V_p^j P_j^l \cdot P_r^s V_s^k P_k^r \cdot \delta_{jp} \delta_{im} \delta_{ln} \cdot \delta_{iq} \cdot \delta_{kr} \cdot \delta_{ks}, \quad (23)$$

$$L(AS)_3[i, j, k, l] = D_q H_n^{pm} P_p^n P_m^q \cdot P_n^p V_l^n P_j^l \cdot P_s^k V_r^s P_k^r \cdot \delta_{jp} \delta_{im} \delta_{ln} \cdot \delta_{iq} \cdot \delta_{kr} \cdot \delta_{ks}, \quad (24)$$

$$L(AS)_4[i, j, k, l] = D_q H_n^{pm} P_p^n P_m^q \cdot P_n^p V_p^j P_j^l \cdot P_s^k V_r^s P_k^r \cdot \delta_{jp} \delta_{im} \delta_{ln} \cdot \delta_{iq} \cdot \delta_{kr} \cdot \delta_{ks}, \quad (25)$$

$$L(AS)_5[i, j, k, l] = D_q H_n^{pm} P_p^n P_m^q \cdot P_n^p V_l^n P_j^l \cdot P_q^m V_r^k P_k^r \cdot \delta_{jp} \delta_{im} \delta_{ln} \cdot \delta_{iq} \cdot \delta_{kr}, \quad (26)$$

$$L(AS)_6[i, j, k, l] = D_q H_n^{pm} P_p^n P_m^q \cdot P_n^p V_p^j P_j^l \cdot P_q^m V_r^k P_k^r \cdot \delta_{jp} \delta_{im} \delta_{ln} \cdot \delta_{iq} \cdot \delta_{kr}, \quad (27)$$

$$L(AS)_7[i, j, k, l] = D_q H_n^{pm} P_p^n P_m^q \cdot P_n^p V_l^n P_j^l \cdot P_q^m V_m^q P_k^k \cdot \delta_{jp} \delta_{im} \delta_{ln} \cdot \delta_{iq}, \quad (28)$$

$$L(AS)_8[i, j, k, l] = D_q H_n^{pm} P_p^n P_m^q \cdot P_n^p V_p^j P_j^l \cdot P_q^m V_m^q P_k^k \cdot \delta_{jp} \delta_{im} \delta_{ln} \cdot \delta_{iq}, \quad (29)$$

$$L(AS)_9[i, j, k, l] = D_q H_n^{pm} P_p^n P_m^q \cdot P_n^p V_p^n P_k^k \cdot P_q^m V_l^j P_j^l \cdot \delta_{jp} \delta_{im} \delta_{ln} \cdot \delta_{iq}. \quad (30)$$

$T \Rightarrow P$ :

$$L(P)[i, j, k, l] = D_q H_n^{pm} P_p^n P_m^q \cdot P_n^p V_j^n P_k^j \cdot P_q^m V_m^j P_j^i \cdot \delta_{kp} \delta_{lm} \delta_{ln} \cdot \delta_{iq}. \quad (31)$$

$T \Rightarrow PS$

$$L(PS)_1[i, j, k, l] = D_q H_n^{pm} P_p^n P_m^q \cdot P_n^p V_i^n P_j^i \cdot P_q^m V_m^q P_k^k \cdot \delta_{jp} \delta_{lm} \delta_{ln} \cdot \delta_{iq}, \quad (32)$$

$$L(PS)_2[i, j, k, l] = D_q H_n^{pm} P_p^n P_m^q \cdot P_n^p V_p^n P_k^k \cdot P_q^m V_m^j P_j^i \cdot \delta_{jp} \delta_{lm} \delta_{ln} \cdot \delta_{iq}. \quad (33)$$

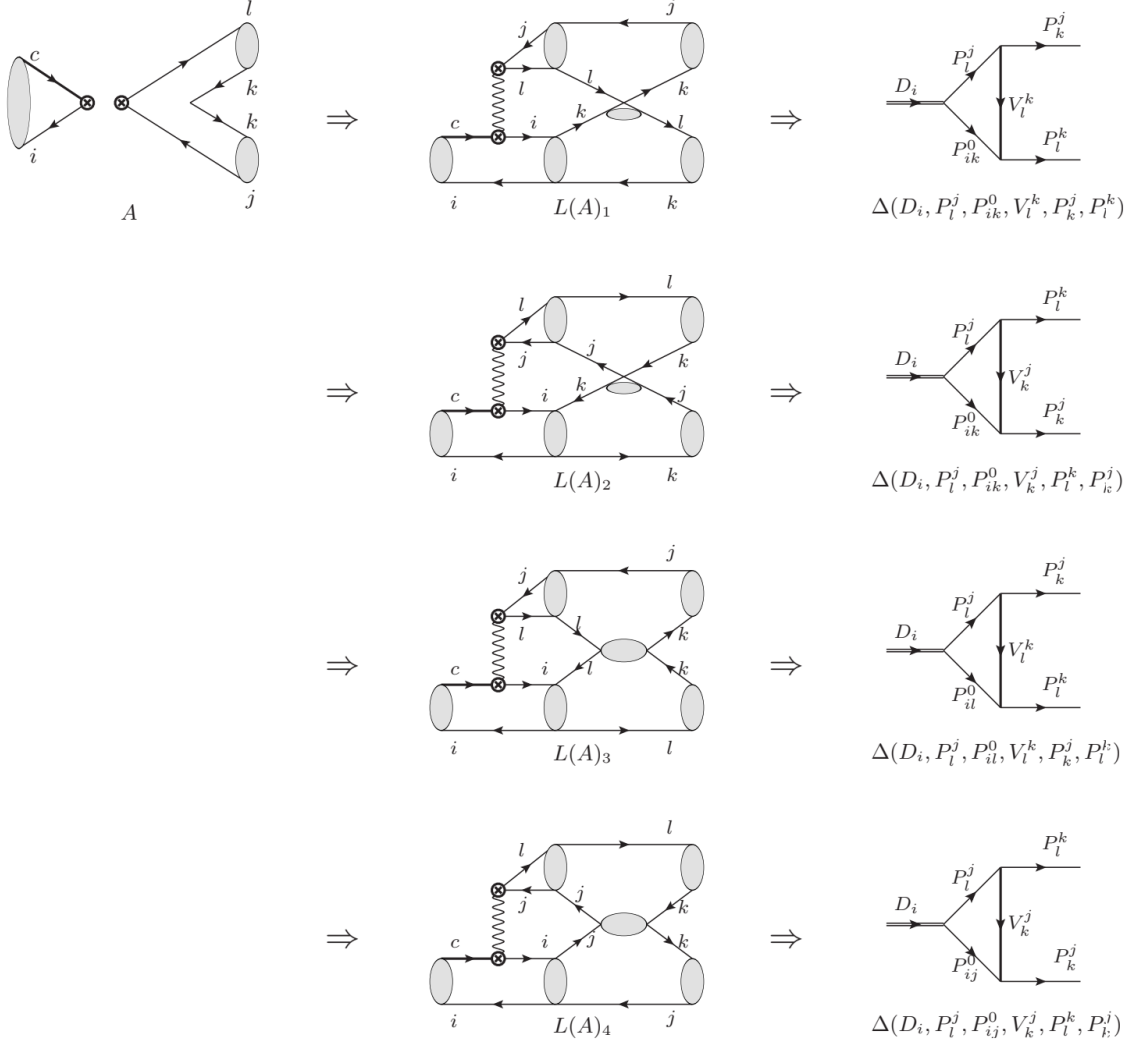


FIG. 8: Topological diagram  $\Rightarrow$  Quark diagram  $\Rightarrow$  Triangle diagram in  $T \Rightarrow A$  transition.

$T \Rightarrow PA$ : no contraction.

$T \Rightarrow SS$ :

$$L(SS)[i, j, k, l] = D_q H_n^{pm} P_p^n P_m^q \cdot P_n^p V_p^n P_j^j \cdot P_q^m V_m^q P_k^k \cdot \delta_{ip} \delta_{lm} \delta_{ln} \cdot \delta_{iq}. \quad (34)$$

Notice that not all the above tensor structures can be understood as triangle diagrams. For example,  $L(ES)_1$  cannot form a triangle diagram at hadron level because  $P_q^m V_m^q P_k^k$  is not an effective strong vertex like Fig. 5. The triangle diagrams constructed by the quark diagrams in  $T \Rightarrow A$ ,  $T \Rightarrow AS$  and  $T \Rightarrow P$  transitions are presented in Figs. 8, 9 and 10 respectively.

The triangle diagrams in the  $T \Rightarrow AS$  transition cancel each other. In Fig. 9, the triangle diagrams derived by quark diagrams  $L(AS)_1$  and  $L(AS)_3$  are the same. But there is a cross in the quark diagram  $L(AS)_3$ , which leads to a minus in the triangle diagram, and hence  $L(AS)_1 +$

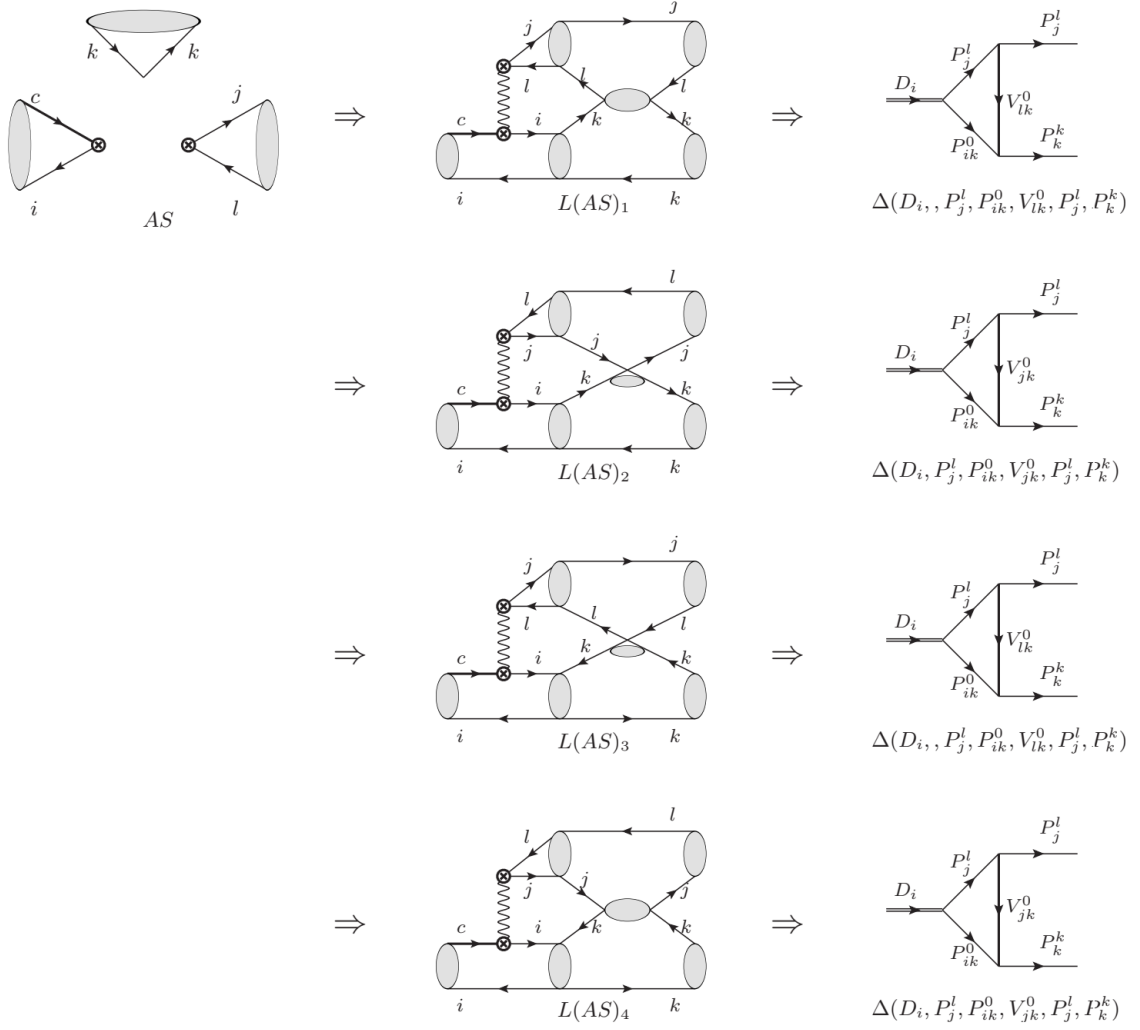


FIG. 9: Topological diagram  $\Rightarrow$  Quark diagram  $\Rightarrow$  Triangle diagram in  $T \Rightarrow AS$  transition.

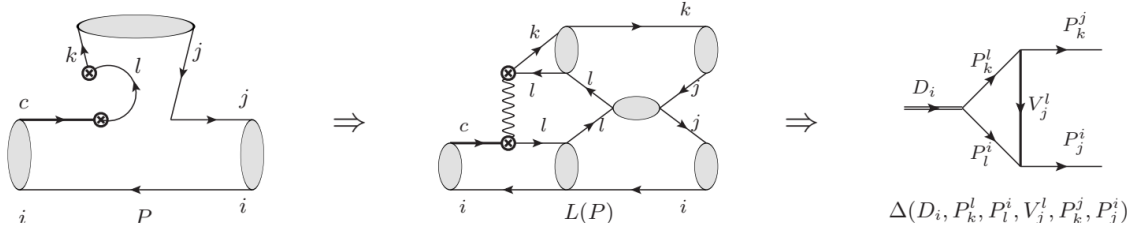


FIG. 10: Topological diagram  $\Rightarrow$  Quark diagram  $\Rightarrow$  Triangle diagram in  $T \Rightarrow P$  transition.

$L(AS)_3 = 0$ . The same situation also appears in the quark diagrams  $L(AS)_2$  and  $L(AS)_4$ . Thereby, the triangle diagrams associated with  $T \Rightarrow AS$  transition do not contribute.

The meson-meson scattering in the  $C$ ,  $E$  and  $P$  diagrams is sketched by  $S_1$  in Fig. 11. And the scattering in the  $T$  diagram and  $A$  diagram are sketched by  $S_2$  and  $S_3$  respectively. Specifically,

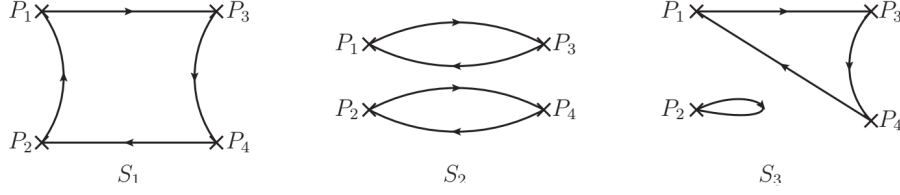


FIG. 11: Sketches of meson-meson scattering in the rescattering contributions of  $C$ ,  $E$ ,  $P$  diagrams (left),  $T$  diagram (middle) and  $A$  diagram (right).

diagram  $S_1$  in Fig. 11 is the meson-meson scattering in  $T \Rightarrow P$  transition, Fig. 10. Flipping the direction of quark lines of  $S_1$ , one can get the meson-meson scattering in  $T \Rightarrow E$  transition, Fig. 2. Twisting the quark lines of  $S_1$  and its flipping to interchange the position of  $P_3$  and  $P_4$ , one can get the meson-meson scattering in  $T \Rightarrow C$  transition, Fig. 4. Thereby, all the four possible topological structures of  $S_1$  are included in the quark diagrams in  $T \Rightarrow E$ ,  $C$ ,  $P$  transitions. For the  $S_2$  diagram in Fig. 11, we can tab the four quark lines with 1, 2, 3, 4 orderly. The intermediate vector propagators of the four quark diagrams in Fig. 6 are formed by the 24, 14, 23, 13 quark lines of  $S_2$  in turn. All the four possible topological structures of  $S_2$  are included in the four quark diagrams in  $T \Rightarrow T$  transition. The  $S_3$  diagram in Fig. 11 is the meson-meson scattering of the fourth quark diagram in Fig. 8. Flipping the direction of quark lines of the above sub-diagram of  $S_3$ , we get the meson-meson scattering of the third quark diagram in Fig. 8. Twisting the quark lines of the above sub-diagram of  $S_3$  and its flipping to interchange the position of  $P_3$  and  $P_4$ , we get the meson-meson scattering of the first two quark diagram in Fig. 8. And again, all the four possible structures of  $S_3$  are included in the four quark diagrams in  $T \Rightarrow A$  transition. In the end, the quark diagrams in  $T \Rightarrow T$ ,  $T \Rightarrow C$ ,  $T \Rightarrow E$ ,  $T \Rightarrow A$  and  $T \Rightarrow P$  transitions cover all the twelve possible topological structures of meson-meson scattering without repetition. So Fig. 11 helps us make clear the completeness of quark diagram.

The rescattering contributions can also be constructed by the two mesons emitted from the short-distance  $C$  diagram,  $C^{SD}$ . In the quark diagram, it is equivalent to use the short-distance  $C$  diagram to replace the short-distance  $T$  diagram. For example, the quark diagram of  $C \Rightarrow A$  transition  $L'(A)$  can be obtained from the quark diagram of  $T \Rightarrow E$  transition  $L(E)$ , see Fig. 12. The relations between the quark diagrams arisen from  $C^{SD}$  and  $T^{SD}$  are summarized to be

$$\begin{aligned} L'(C_i) &= \frac{C^{SD}}{T^{SD}} L(T_i), & L'(A) &= \frac{C^{SD}}{T^{SD}} L(E), & L'(T_i) &= \frac{C^{SD}}{T^{SD}} L(C_i), \\ L'(E_i) &= \frac{C^{SD}}{T^{SD}} L(A_i), & L'(P') &= \frac{C^{SD}}{T^{SD}} L(P), \end{aligned} \quad (35)$$

in which  $P'$  diagram is the Fierz transformation of  $P$  diagram. In the SM,  $P'$  diagram is zero if

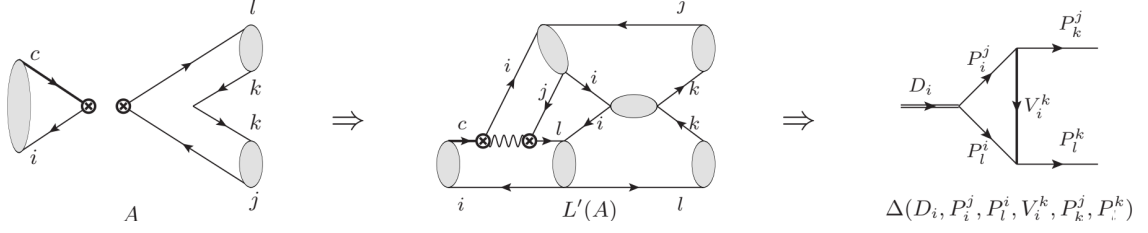


FIG. 12: Topological diagram  $\Rightarrow$  Quark diagram  $\Rightarrow$  Triangle diagram in  $C \Rightarrow A$  transition.

the tree operators  $O_1$  or  $Q_2$  is inserted into its weak vertex. The ratio  $C^{SD}/T^{SD}$  in Eq. (35) is suppressed by the color factor at charm scale [23]

$$\frac{C_1(m_c) + C_2(m_c)/3}{C_2(m_c) + C_1(m_c)/3} \sim \mathcal{O}(10^{-2 \sim -1}). \quad (36)$$

Thus the rescattering contributions arisen from  $C^{SD}$  are about one order smaller than ones arisen from  $T^{SD}$ . In addition, the short-distance  $E$ ,  $A$  and  $P$  diagrams are deeply suppressed by the helicity suppression or the small running coupling constant  $\alpha(\mu)$ . The rescattering contributions arisen from  $E^{SD}$ ,  $A^{SD}$  and  $P^{SD}$  are negligible.

The  $ES$ ,  $AS$ ,  $PS$ ,  $PA$  and  $SS$  diagrams can be divided into several unconnected parts by cutting off gluon propagators. They are suppressed by the OZI rule [50–52] and can not be constructed by scattering of the two mesons generated by a short-distance diagram. On the contrary, the  $T$ ,  $C$ ,  $E$ ,  $A$  and  $P$  diagrams cannot be divided into unconnected sub-diagram by cutting off gluon propagators and hence their long-distance contributions could be modeled into meson-meson scattering.

For convenience to the subsequent analysis, we factor out the coefficient of constituent quarks of meson in the triangle diagram. For example, the  $u\bar{u}$  constituent for pseudoscalar meson can be written as  $1/\sqrt{2}\pi^0 + 1/\sqrt{6}\eta_8 + 1/\sqrt{3}\eta_1$ . If a  $\pi^0$  with  $u\bar{u}$  constituent emits as a final state, the factor  $1/\sqrt{2}$  is multiplied before the triangle diagram. If the  $u\bar{u}$  constituent acts as a propagator, the propagator should be written as  $\pi^0/2 + \eta_8/6 + \eta_1/3$  since there are two effective vertexes at triangle diagram. In this way, all triangle diagrams are equivalent under the  $SU(3)_F$  symmetry.

Under the  $SU(3)_F$  symmetry, the rescattering contributions arisen from  $T^{SD}$  in the  $T$  and  $A$  diagrams are zero because of the neutral propagators constructed by dyadic tensors. For example, if  $i = u$ ,  $k = d$  in  $L(T)_1$ , the vector propagator  $V_{ik}^0$  is  $-\rho^0/2 + \omega/2$ . Under the  $SU(3)_F$  symmetry,  $\rho^0 = \omega$ , and hence  $L(T)_1 = 0$ . This situation also appears in other quark diagrams of  $T$  and  $A$  diagrams. Thereby, the rescattering contributions arisen from  $T^{SD}$  in the  $T$  and  $A$  diagrams are only induced by the  $SU(3)_F$  breaking effects. The dyadic tensors do not appear in  $T \Rightarrow E$ ,  $T \Rightarrow C$  and  $T \Rightarrow P$  transitions. Considering the  $C^{SD}$  amplitude is one order smaller than the  $T^{SD}$

amplitude, the rescattering contributions in the  $T$  and  $A$  diagrams are smaller than  $C$ ,  $E$  and  $P$  diagrams. The different size between rescattering contributions in the  $T$ ,  $A$  diagrams and the  $C$ ,  $E$  and  $P$  diagrams can be understood in the large  $N_c$  expansion. In Fig. 11,  $S_1$  is a color singlet. It is at order of  $(1/\sqrt{N_c})^4 N_c = 1/N_c$  in the large  $N_c$  expansion.  $S_2$  and  $S_3$  include two color singlets. They are at order of  $(1/\sqrt{N_c})^4 (N_c)^2 / (N_c)^2 = 1/N_c^2$  in the large  $N_c$  expansion.

Considering that there are two quark diagrams in  $T \Rightarrow C$  transition and one quark diagram in  $T \Rightarrow E$  and  $T \Rightarrow P$  transitions as well as the minus sign induced by the cross of quark lines in the quark diagrams in  $T \Rightarrow C$  transition, we conclude that

$$L(C) : L(E) : L(P) = -2 : 1 : 1 \quad (37)$$

in the  $SU(3)_F$  symmetry. Since  $C^{SD}$  is one order smaller than  $T^{SD}$ , Eq. (37) will not be obviously broken if other rescattering contributions are included. If the resonances are considered, Eq. (37) is broken. But the proportional relation is still significant since it gives a rough estimation of the long-distance contributions. One can find the rescattering contribution in  $P$  diagram is at the same order with  $C$  and  $E$  diagrams. It is consistent with the large penguin diagram extracted from CP violation in charm decay [53, 54]. In Ref. [19], the authors assumed  $PE = E$  and predicted that  $\Delta A_{CP} = (-1.39 \pm 0.04) \times 10^{-3}$  or  $(-1.51 \pm 0.04) \times 10^{-3}$ , very close to the experimental value,  $\Delta A_{CP} = (-1.54 \pm 0.29) \times 10^{-3}$  [53]. In fact, the assumptions that  $PE = E$ ,  $P = E$  or  $P + PE = E$  will give similar results because  $P$  and  $PE$  defined in [19] always appear as  $P + PE$ . In Ref. [34], we conclude that topology  $P$  defined in this work is identical to  $P + PE$  defined in [19]. So  $L(P) = L(E)$  is consistent with the hypothesis proposed in [19].

### III. APPLICATION IN $D$ MESON DECAY

In this section, we take the  $D \rightarrow K\pi$  and  $D \rightarrow \pi\pi$  decays as examples to illustrate the reliability of the theoretical framework. We only analyze the rescattering contributions arisen from  $T^{SD}$  since the rescattering contributions arisen from other short-distance amplitudes are suppressed.

### A. $D \rightarrow K\pi$ decay

The topological amplitude of  $D^0 \rightarrow K^- \pi^+$  decay is  $T + E$ . The long-distance contributions modeled by triangle diagram at hadron level include

$$L(T)_1[u, s, d, u] = \frac{1}{2}\Delta(D^0, \pi^+, K^-, \rho^0, \pi^+, K^-) - \frac{1}{2}\Delta(D^0, \pi^+, K^-, \omega, \pi^+, K^-), \quad (38)$$

$$L(E)[u, d, u, s] = \frac{1}{2}\Delta(D^0, \pi^+, K^-, \rho^0, \pi^+, K^-) + \frac{1}{2}\Delta(D^0, \pi^+, K^-, \omega, \pi^+, K^-). \quad (39)$$

After summing the  $T$  and  $E$  amplitudes, the rescattering amplitude of  $D^0 \rightarrow K^- \pi^+$  is

$$\mathcal{A}_L(D^0 \rightarrow K^- \pi^+) = L(T)_1[u, s, d, u] + L(E)[u, d, u, s] = \Delta(D^0, \pi^+, K^-, \rho^0, \pi^+, K^-). \quad (40)$$

Notice that the contributions associated with  $\omega\pi\pi$  vertex cancel each other. The topological amplitude of  $D^0 \rightarrow \bar{K}^0 \pi^0$  decay is  $\frac{1}{\sqrt{2}}C - \frac{1}{\sqrt{2}}E$ . The rescattering contributions include

$$\frac{1}{\sqrt{2}}L(C)_1[u, u, d, s] = -\frac{1}{\sqrt{2}}\Delta(D^0, \pi^+, K^-, \rho^+, \pi^0, \bar{K}^0), \quad (41)$$

$$\frac{1}{\sqrt{2}}L(C)_2[u, u, d, s] = -\frac{1}{\sqrt{2}}\Delta(D^0, \pi^+, K^-, K^{*+}, \bar{K}^0, \pi^0), \quad (42)$$

$$-\frac{1}{\sqrt{2}}L(E)[u, d, d, s] = -\frac{1}{\sqrt{2}}\Delta(D^0, \pi^+, K^-, \rho^+, \pi^0, \bar{K}^0). \quad (43)$$

Summing the  $C$  and  $E$  amplitudes, we have

$$\begin{aligned} \mathcal{A}_L(D^0 \rightarrow \bar{K}^0 \pi^0) &= \frac{1}{\sqrt{2}}L(C)_1[u, u, d, s] + \frac{1}{\sqrt{2}}L(C)_2[u, u, d, s] - \frac{1}{\sqrt{2}}L(E)[u, d, d, s] \\ &= -\sqrt{2}\Delta(D^0, \pi^+, K^-, \rho^+, \pi^0, \bar{K}^0) - \frac{1}{\sqrt{2}}\Delta(D^0, \pi^+, K^-, K^{*+}, \bar{K}^0, \pi^0). \end{aligned} \quad (44)$$

The topological amplitude of  $D^+ \rightarrow \bar{K}^0 \pi^+$  decay is  $T + C$ . The rescattering contributions include

$$L(T)_2[d, s, d, u] = -\frac{1}{2}\Delta(D^+, \pi^+, \bar{K}^0, \rho^0, \pi^+, \bar{K}^0) + \frac{1}{2}\Delta(D^0, \pi^+, \bar{K}^0, \omega, \pi^+, \bar{K}^0), \quad (45)$$

$$L(C)_1[d, u, d, s] = -\frac{1}{2}\Delta(D^+, \pi^+, \bar{K}^0, \rho^0, \pi^+, \bar{K}^0) - \frac{1}{2}\Delta(D^+, \pi^+, \bar{K}^0, \omega, \pi^+, \bar{K}^0), \quad (46)$$

$$L(C)_2[d, u, d, s] = \Delta(D^+, \pi^+, \bar{K}^0, K^{*+}, \bar{K}^0, \pi^+). \quad (47)$$

Summing the  $T$  and  $C$  amplitudes, we have

$$\begin{aligned} \mathcal{A}_L(D^+ \rightarrow \bar{K}^0 \pi^+) &= L(T)_2[d, s, d, u] + L(C)_1[d, u, d, s] + L(C)_2[d, u, d, s] \\ &= -\Delta(D^+, \pi^+, \bar{K}^0, \rho^0, \pi^+, \bar{K}^0) + \Delta(D^+, \pi^+, \bar{K}^0, K^{*+}, \bar{K}^0, \pi^+). \end{aligned} \quad (48)$$

Again, all the contributions associated with  $\omega\pi\pi$  vertex cancel each other.

Eqs. (40), (44) and (48) can also be derived directly from the chiral Lagrangian (9). That is, drawing and calculation the triangle diagram in a Feynman diagram like way with the chiral Lagrangian. Starting from the topological diagrams, we obtain the same results via the quark diagrams. It indicates the inherent correlation between the topological amplitude and the rescattering dynamics. It is understandable since both the topological amplitude and rescattering dynamics are originated from the Quark Model (QM).

Under the Isospin symmetry, the particles in an Isospin multiplet can be seen as the same particles. Then we have

$$\begin{aligned}\Delta_1 &= \Delta(D^0, \pi^+, K^-, \rho^0, \pi^+, K^-) = \Delta(D^0, \pi^+, K^-, \rho^+, \pi^0, \bar{K}^0) = \Delta(D^+, \pi^+, \bar{K}^0, \rho^0, \pi^+, \bar{K}^0), \\ \Delta_2 &= \Delta(D^0, \pi^+, K^-, K^{*+}, \bar{K}^0, \pi^0) = \Delta(D^+, \pi^+, \bar{K}^0, K^{*+}, \bar{K}^0, \pi^+).\end{aligned}\quad (49)$$

The decay amplitudes of  $D^+ \rightarrow \bar{K}^0 \pi^+$ ,  $D^0 \rightarrow \bar{K}^0 \pi^0$  and  $D^0 \rightarrow K^- \pi^+$  channels can be written as

$$\begin{aligned}\mathcal{A}_L(D^+ \rightarrow \bar{K}^0 \pi^+) &= -\Delta_1 - \Delta_2, & \mathcal{A}_L(D^0 \rightarrow \bar{K}^0 \pi^0) &= -\sqrt{2}\Delta_1 - \frac{1}{\sqrt{2}}\Delta_2, \\ \mathcal{A}_L(D^0 \rightarrow K^- \pi^+) &= \Delta_1.\end{aligned}\quad (50)$$

One can check the Isospin relation

$$\mathcal{A}(D^+ \rightarrow \bar{K}^0 \pi^+) - \mathcal{A}(D^0 \rightarrow K^- \pi^+) = \sqrt{2}\mathcal{A}(D^0 \rightarrow \bar{K}^0 \pi^0) \quad (51)$$

is satisfied in terms of the triangle diagrams.

The rescattering contributions of  $T$  amplitude in the  $D^0 \rightarrow K^- \pi^+$  and  $D^+ \rightarrow \bar{K}^0 \pi^+$  decays are different under the Isospin symmetry, see Eq. (38) and Eq. (45). In a higher flavor symmetry, the  $SU(3)_F$  symmetry, the equivalence of  $T$  diagram in the  $D^0 \rightarrow K^- \pi^+$  and  $D^+ \rightarrow \bar{K}^0 \pi^+$  decays regained due to  $\rho = \omega$ . Above discussion also applies to  $C$  and  $E$  diagrams. It means the relation  $L(C) = -2L(E)$  only holds in the  $SU(3)_F$  symmetry but not in the Isospin symmetry. The Isospin amplitudes of the  $D^0 \rightarrow K^- \pi^+$ ,  $D^0 \rightarrow \bar{K}^0 \pi^0$  and  $D^+ \rightarrow \bar{K}^0 \pi^+$  decays are

$$\begin{aligned}\mathcal{A}(D^+ \rightarrow \bar{K}^0 \pi^+) &= \frac{1}{3}\mathcal{A}_{3/2} + \frac{2}{3}\mathcal{A}_{1/2}, & \mathcal{A}(D^0 \rightarrow \bar{K}^0 \pi^0) &= \frac{\sqrt{2}}{3}(\mathcal{A}_{3/2} - \mathcal{A}_{1/2}), \\ \mathcal{A}(D^0 \rightarrow K^- \pi^+) &= \mathcal{A}_{3/2}.\end{aligned}\quad (52)$$

Notice that there are only two Isospin amplitudes. The number of Isospin amplitude does not equal to the topological amplitude. Thus the topological amplitudes cannot be expressed by Isospin amplitudes. The topological amplitudes  $T$ ,  $C$  and  $E$  need not be equivalent respectively in different decay channels if only the Isospin symmetry is maintained.



## B. $D \rightarrow \pi\pi$ decay

The topological amplitude of  $D^0 \rightarrow \pi^+\pi^-$  decay is  $\lambda_d(T + E) + \lambda_d(P + 2PA) + \lambda_s(P + 2PA)$ , in which  $\lambda_d = V_{cd}^*V_{ud}$  and  $\lambda_s = V_{cs}^*V_{us}$ . The rescattering contributions in the  $D^0 \rightarrow \pi^+\pi^-$  decay modeled by triangle diagram include

$$\lambda_d L(T)_1[u, d, d, u] = \frac{1}{2}\lambda_d \Delta(D^0, \pi^+, \pi^-, \rho^0, \pi^+, \pi^-) - \frac{1}{2}\lambda_d \Delta(D^0, \pi^+, \pi^-, \omega, \pi^+, \pi^-), \quad (53)$$

$$\lambda_d L(T)_4[u, d, d, u] = \frac{1}{2}\lambda_d \Delta(D^0, \pi^+, \pi^-, \rho^0, \pi^+, \pi^-) - \frac{1}{2}\lambda_d \Delta(D^0, \pi^+, \pi^-, \omega, \pi^+, \pi^-), \quad (54)$$

$$\lambda_d L(E)[u, d, u, d] = \frac{1}{2}\lambda_d \Delta(D^0, \pi^+, \pi^-, \rho^0, \pi^+, \pi^-) + \frac{1}{2}\lambda_d \Delta(D^0, \pi^+, \pi^-, \omega, \pi^+, \pi^-), \quad (55)$$

$$\lambda_d L(P)[u, d, u, d] = \frac{1}{2}\lambda_d \Delta(D^0, \pi^+, \pi^-, \rho^0, \pi^+, \pi^-) + \frac{1}{2}\lambda_d \Delta(D^0, \pi^+, \pi^-, \omega, \pi^+, \pi^-), \quad (56)$$

$$\lambda_s L(P)[u, d, u, s] = \lambda_s \Delta(D^0, K^+, K^-, K^{*0}, \pi^+, \pi^-). \quad (57)$$

Summing all of them, the rescattering amplitude in the  $D^0 \rightarrow \pi^+\pi^-$  decay is

$$\begin{aligned} \mathcal{A}_L(D^0 \rightarrow \pi^+\pi^-) &= \lambda_d(L(T)_1[u, d, d, u] + L(T)_4[u, d, d, u] + L(E)[u, d, u, d] \\ &\quad + L(P)[u, d, u, d]) + \lambda_s L(P)[u, d, u, s] \\ &= 2\lambda_d \Delta(D^0, \pi^+, \pi^-, \rho^0, \pi^+, \pi^-) + \lambda_s \Delta(D^0, K^+, K^-, K^{*0}, \pi^+, \pi^-). \end{aligned} \quad (58)$$

The topological amplitude of  $D^0 \rightarrow \pi^0\pi^0$  decay is  $\frac{1}{\sqrt{2}}\lambda_d(E - C) + \frac{1}{\sqrt{2}}\lambda_d(P + 2PA) + \frac{1}{\sqrt{2}}\lambda_s(P + 2PA)$ .

The rescattering contributions in the  $D^0 \rightarrow \pi^0\pi^0$  decay include

$$\frac{1}{\sqrt{2}}\lambda_d L(E)[u, d, d, d] = \frac{1}{\sqrt{2}}\lambda_d \Delta(D^0, \pi^+, \pi^-, \rho^+, \pi^0, \pi^0), \quad (59)$$

$$-\frac{1}{\sqrt{2}}\lambda_d L(C)_1[u, u, d, d] = \frac{1}{\sqrt{2}}\lambda_d \Delta(D^0, \pi^+, \pi^-, \rho^+, \pi^0, \pi^0), \quad (60)$$

$$-\frac{1}{\sqrt{2}}\lambda_d L(C)_2[u, u, d, d] = \frac{1}{\sqrt{2}}\lambda_d \Delta(D^0, \pi^+, \pi^-, \rho^+, \pi^0, \pi^0), \quad (61)$$

$$\frac{1}{\sqrt{2}}\lambda_d L(P)[u, u, u, d] = \frac{1}{\sqrt{2}}\lambda_d \Delta(D^0, \pi^+, \pi^-, \rho^+, \pi^0, \pi^0), \quad (62)$$

$$\frac{1}{\sqrt{2}}\lambda_s L(P)[u, u, u, s] = \frac{1}{\sqrt{2}}\lambda_s \Delta(D^0, K^+, K^-, K^{*+}, \pi^0, \pi^0). \quad (63)$$

Summing all of them, the rescattering amplitude in the  $D^0 \rightarrow \pi^0\pi^0$  decay is

$$\begin{aligned} \mathcal{A}_L(D^0 \rightarrow \pi^0\pi^0) &= \frac{1}{\sqrt{2}}\lambda_d(L(E)[u, d, d, d] - L(C)_1[u, u, d, d] - L(C)_2[u, u, d, d] \\ &\quad + L(P)[u, u, u, d]) + \frac{1}{\sqrt{2}}\lambda_s L(P)[u, u, u, s] \\ &= 2\sqrt{2}\lambda_d \Delta(D^0, \pi^+, \pi^-, \rho^+, \pi^0, \pi^0) + \frac{1}{\sqrt{2}}\lambda_s \Delta(D^0, K^+, K^-, K^{*+}, \pi^0, \pi^0). \end{aligned} \quad (64)$$

The topological amplitude of  $D^+ \rightarrow \pi^+ \pi^0$  decay is  $-\frac{1}{\sqrt{2}}\lambda_d(T+C)$ . The rescattering contributions in the  $D^+ \rightarrow \pi^+ \pi^0$  decay include

$$\begin{aligned}
-\frac{1}{\sqrt{2}}\lambda_d L(T)_2[d, d, u, d] &= \frac{1}{4\sqrt{2}}\lambda_d \Delta(D^+, \pi^+, \pi^0, \rho^0, \pi^+, \pi^0) + \frac{1}{12\sqrt{2}}\lambda_d \Delta(D^0, \pi^+, \eta_8, \rho^0, \pi^+, \pi^0) \\
&+ \frac{1}{6\sqrt{2}}\lambda_d \Delta(D^+, \pi^+, \eta_1, \rho^0, \pi^+, \pi^0) - \frac{1}{4\sqrt{2}}\lambda_d \Delta(D^+, \pi^+, \pi^0, \omega, \pi^+, \pi^0) \\
&- \frac{1}{12\sqrt{2}}\lambda_d \Delta(D^0, \pi^+, \eta_8, \omega, \pi^+, \pi^0) - \frac{1}{6\sqrt{2}}\lambda_d \Delta(D^+, \pi^+, \eta_1, \omega, \pi^+, \pi^0),
\end{aligned} \tag{65}$$

$$\begin{aligned}
-\frac{1}{\sqrt{2}}\lambda_d L(T)_4[d, d, u, d] &= -\frac{1}{4\sqrt{2}}\lambda_d \Delta(D^+, \pi^+, \pi^0, \rho^0, \pi^+, \pi^0) - \frac{1}{12\sqrt{2}}\lambda_d \Delta(D^0, \pi^+, \eta_8, \rho^0, \pi^+, \pi^0) \\
&= -\frac{1}{6\sqrt{2}}\lambda_d \Delta(D^+, \pi^+, \eta_1, \rho^0, \pi^+, \pi^0) + \frac{1}{4\sqrt{2}}\lambda_d \Delta(D^+, \pi^+, \pi^0, \omega, \pi^+, \pi^0) \\
&+ \frac{1}{12\sqrt{2}}\lambda_d \Delta(D^0, \pi^+, \eta_8, \omega, \pi^+, \pi^0) + \frac{1}{6\sqrt{2}}\lambda_d \Delta(D^+, \pi^+, \eta_1, \omega, \pi^+, \pi^0),
\end{aligned} \tag{66}$$

$$\begin{aligned}
-\frac{1}{\sqrt{2}}\lambda_d L(C)_1[d, u, d, d] &= \frac{1}{4\sqrt{2}}\lambda_d \Delta(D^+, \pi^+, \pi^0, \rho^0, \pi^+, \pi^0) + \frac{1}{12\sqrt{2}}\lambda_d \Delta(D^0, \pi^+, \eta_8, \rho^0, \pi^+, \pi^0) \\
&+ \frac{1}{6\sqrt{2}}\lambda_d \Delta(D^+, \pi^+, \eta_1, \rho^0, \pi^+, \pi^0) + \frac{1}{4\sqrt{2}}\lambda_d \Delta(D^+, \pi^+, \pi^0, \omega, \pi^+, \pi^0) \\
&+ \frac{1}{12\sqrt{2}}\lambda_d \Delta(D^0, \pi^+, \eta_8, \omega, \pi^+, \pi^0) + \frac{1}{6\sqrt{2}}\lambda_d \Delta(D^+, \pi^+, \eta_1, \omega, \pi^+, \pi^0),
\end{aligned} \tag{67}$$

$$\begin{aligned}
-\frac{1}{\sqrt{2}}\lambda_d L(C)_2[d, u, d, d] &= \frac{1}{2\sqrt{2}}\lambda_d \Delta(D^+, \pi^+, \pi^0, \rho^+, \pi^0, \pi^+) + \frac{1}{6\sqrt{2}}\lambda_d \Delta(D^0, \pi^+, \eta_8, \rho^+, \pi^0, \pi^+) \\
&+ \frac{1}{3\sqrt{2}}\lambda_d \Delta(D^+, \pi^+, \eta_1, \rho^+, \pi^0, \pi^+).
\end{aligned} \tag{68}$$

Topology  $A$  does not contribute to the  $D^+ \rightarrow \pi^+ \pi^0$  decay in the  $SU(3)_F$  symmetry because of the cancellation between  $u\bar{u}$  and  $d\bar{d}$  generated via gluons. In order to get completed rescattering contributions, the quark diagrams in the  $T \Rightarrow A$  transition should be considered. The rescattering

contributions in  $A$  diagram are

$$\begin{aligned}
\frac{1}{\sqrt{2}}\lambda_d L(A)_1[d, d, u, u] &= \frac{1}{4\sqrt{2}}\lambda_d \Delta(D^+, \pi^+, \pi^0, \rho^0, \pi^+, \pi^0) - \frac{1}{12\sqrt{2}}\lambda_d \Delta(D^0, \pi^+, \eta_8, \rho^0, \pi^+, \pi^0) \\
&\quad - \frac{1}{6\sqrt{2}}\lambda_d \Delta(D^+, \pi^+, \eta_1, \rho^0, \pi^+, \pi^0) + \frac{1}{4\sqrt{2}}\lambda_d \Delta(D^+, \pi^+, \pi^0, \omega, \pi^+, \pi^0) \\
&\quad - \frac{1}{12\sqrt{2}}\lambda_d \Delta(D^0, \pi^+, \eta_8, \omega, \pi^+, \pi^0) - \frac{1}{6\sqrt{2}}\lambda_d \Delta(D^+, \pi^+, \eta_1, \omega, \pi^+, \pi^0),
\end{aligned} \tag{69}$$

$$\begin{aligned}
\frac{1}{\sqrt{2}}\lambda_d L(A)_2[d, d, u, u] &= \frac{1}{2\sqrt{2}}\lambda_d \Delta(D^+, \pi^+, \pi^0, \rho^+, \pi^0, \pi^+) - \frac{1}{6\sqrt{2}}\lambda_d \Delta(D^0, \pi^+, \eta_8, \rho^+, \pi^0, \pi^+) \\
&\quad - \frac{1}{3\sqrt{2}}\lambda_d \Delta(D^+, \pi^+, \eta_1, \rho^+, \pi^0, \pi^+),
\end{aligned} \tag{70}$$

$$\begin{aligned}
\frac{1}{\sqrt{2}}\lambda_d L(A)_3[d, d, u, u] &= -\frac{1}{4\sqrt{2}}\lambda_d \Delta(D^+, \pi^+, \pi^0, \rho^0, \pi^+, \pi^0) + \frac{1}{12\sqrt{2}}\lambda_d \Delta(D^0, \pi^+, \eta_8, \rho^0, \pi^+, \pi^0) \\
&\quad + \frac{1}{6\sqrt{2}}\lambda_d \Delta(D^+, \pi^+, \eta_1, \rho^0, \pi^+, \pi^0) - \frac{1}{4\sqrt{2}}\lambda_d \Delta(D^+, \pi^+, \pi^0, \omega, \pi^+, \pi^0) \\
&\quad + \frac{1}{12\sqrt{2}}\lambda_d \Delta(D^0, \pi^+, \eta_8, \omega, \pi^+, \pi^0) + \frac{1}{6\sqrt{2}}\lambda_d \Delta(D^+, \pi^+, \eta_1, \omega, \pi^+, \pi^0),
\end{aligned} \tag{71}$$

$$\begin{aligned}
-\frac{1}{\sqrt{2}}\lambda_d L(A)_3[d, d, d, u] &= \frac{1}{2\sqrt{2}}\lambda_d \Delta(D^+, \pi^+, \pi^0, \rho^+, \pi^0, \pi^+) - \frac{1}{6\sqrt{2}}\lambda_d \Delta(D^0, \pi^+, \eta_8, \rho^+, \pi^0, \pi^+) \\
&\quad - \frac{1}{3\sqrt{2}}\lambda_d \Delta(D^+, \pi^+, \eta_1, \rho^+, \pi^0, \pi^+).
\end{aligned} \tag{72}$$

Similar to  $A$  diagram, the rescattering contributions in  $P$  diagram should also be considered:

$$\begin{aligned}
\frac{1}{\sqrt{2}}\lambda_d L(P)[d, u, u, d] &= \frac{1}{2\sqrt{2}}\lambda_d \Delta(D^+, \pi^+, \pi^0, \rho^+, \pi^0, \pi^+) + \frac{1}{6\sqrt{2}}\lambda_d \Delta(D^0, \pi^+, \eta_8, \rho^+, \pi^0, \pi^+) \\
&\quad + \frac{1}{3\sqrt{2}}\lambda_d \Delta(D^+, \pi^+, \eta_1, \rho^+, \pi^0, \pi^+),
\end{aligned} \tag{73}$$

$$\begin{aligned}
-\frac{1}{\sqrt{2}}\lambda_d L(P)[d, d, u, d] &= -\frac{1}{4\sqrt{2}}\lambda_d \Delta(D^+, \pi^+, \pi^0, \rho^0, \pi^+, \pi^0) - \frac{1}{12\sqrt{2}}\lambda_d \Delta(D^0, \pi^+, \eta_8, \rho^0, \pi^+, \pi^0) \\
&\quad - \frac{1}{6\sqrt{2}}\lambda_d \Delta(D^+, \pi^+, \eta_1, \rho^0, \pi^+, \pi^0) - \frac{1}{4\sqrt{2}}\lambda_d \Delta(D^+, \pi^+, \pi^0, \omega, \pi^+, \pi^0) \\
&\quad - \frac{1}{12\sqrt{2}}\lambda_d \Delta(D^0, \pi^+, \eta_8, \omega, \pi^+, \pi^0) - \frac{1}{6\sqrt{2}}\lambda_d \Delta(D^+, \pi^+, \eta_1, \omega, \pi^+, \pi^0),
\end{aligned} \tag{74}$$

$$\frac{1}{\sqrt{2}}\lambda_s L(P)[d, u, u, s] = \frac{1}{\sqrt{2}}\lambda_s \Delta(D^0, K^+, \bar{K}^0, K^{*+}, \pi^0, \pi^+), \tag{75}$$

$$-\frac{1}{\sqrt{2}}\lambda_s L(P)[d, d, u, s] = -\frac{1}{\sqrt{2}}\lambda_s \Delta(D^0, K^+, \bar{K}^0, K^{*0}, \pi^+, \pi^0). \tag{76}$$

Summing all quark diagrams, the rescattering amplitude in the  $D^+ \rightarrow \pi^+ \pi^0$  decay is

$$\begin{aligned}
\mathcal{A}_L(D^+ \rightarrow \pi^+ \pi^0) &= -\frac{1}{\sqrt{2}}\lambda_d(L(T)_2[d, d, u, d] + L(T)_4[d, d, u, d] + L(C)_1[d, u, d, d] \\
&\quad + L(C)_2[d, u, d, d] - L(A)_1[d, d, u, u] - L(A)_2[d, d, u, u] \\
&\quad - L(A)_3[d, d, u, u] + L(A)_3[d, d, d, u] - L(P)[d, u, u, d] \\
&\quad + L(P)[d, d, u, d]) + \frac{1}{\sqrt{2}}\lambda_s(L(P)[d, u, u, s] - L(P)[d, d, u, s]) \\
&= \sqrt{2}\lambda_d\Delta(D^0, \pi^+, \pi^0, \rho^+, \pi^+, \pi^0) + \frac{1}{\sqrt{2}}\lambda_s(\Delta(D^0, K^+, \bar{K}^0, K^{*+}, \pi^0, \pi^+) \\
&\quad - \Delta(D^0, K^+, \bar{K}^0, K^{*0}, \pi^+, \pi^0)). \tag{77}
\end{aligned}$$

Notice that all the contributions with vertexes that not appear in the chiral Lagrangian (9), such as  $\rho^0 \pi^0 \pi^0$ ,  $\rho^0 \eta \eta$  ..., cancel each other.

Eqs. (58), (64) and (77) are consistent with the rescattering amplitudes derived directly from the chiral Lagrangian. Under the Isospin symmetry, we have

$$\begin{aligned}
\Delta_3 &= \Delta(D^0, \pi^+, \pi^-, \rho^0, \pi^+, \pi^-) = \Delta(D^0, \pi^+, \pi^-, \rho^+, \pi^0, \pi^0) = \Delta(D^0, \pi^+, \pi^0, \rho^+, \pi^+, \pi^0), \\
\Delta_4 &= \Delta(D^0, K^+, K^-, K^{*0}, \pi^+, \pi^-) = \Delta(D^0, K^+, K^-, K^{*+}, \pi^0, \pi^0) \\
&= \Delta(D^0, K^+, \bar{K}^0, K^{*+}, \pi^0, \pi^+) = \Delta(D^0, K^+, \bar{K}^0, K^{*0}, \pi^+, \pi^0). \tag{78}
\end{aligned}$$

Then the amplitudes of  $D^0 \rightarrow \pi^+ \pi^-$ ,  $D^0 \rightarrow \pi^0 \pi^0$  and  $D^+ \rightarrow \pi^+ \pi^0$  channels can be written as

$$\begin{aligned}
\mathcal{A}_L(D^0 \rightarrow \pi^+ \pi^-) &= 2\lambda_d\Delta_3 + \lambda_s\Delta_4, \quad \mathcal{A}_L(D^0 \rightarrow \pi^0 \pi^0) = 2\sqrt{2}\lambda_d\Delta_3 + \frac{1}{\sqrt{2}}\lambda_s\Delta_4, \\
\mathcal{A}_L(D^+ \rightarrow \pi^+ \pi^0) &= \sqrt{2}\lambda_d\Delta_3. \tag{79}
\end{aligned}$$

One can check the Isospin relation

$$\mathcal{A}(D^0 \rightarrow \pi^+ \pi^-) - \sqrt{2}\mathcal{A}(D^0 \rightarrow \pi^0 \pi^0) + \sqrt{2}\mathcal{A}(D^+ \rightarrow \pi^+ \pi^0) = 0 \tag{80}$$

is satisfied.

In Ref. [37], the Isospin factor is considered in such a way that the  $u\bar{u}$  component in one final meson  $\pi^0$  contributes a factor of  $1/\sqrt{2}$  and the  $d\bar{d}$  component contributes a factor of  $-1/\sqrt{2}$ . For the intermediate state  $\pi^0$ , the factor  $1/\sqrt{2}$  or  $-1/\sqrt{2}$  is dropped to keep the Isospin relation between the  $D^0 \rightarrow \pi^+ \pi^-$ ,  $D^0 \rightarrow \pi^0 \pi^0$  and  $D^+ \rightarrow \pi^+ \pi^0$  channels. This operation is artificial without sufficient reason. The confusion comes from that not all the quark diagrams are considered in [37]. In this work, the complete quark diagrams contributing to the three channels are found via the tensor form of quark diagram. The Isospin factor is derived directly from quark diagram. For the

neutral meson serving an intermediate state, the Isospin factor is multiplied two times because of the two vertexes. Summing all the quark diagrams, the Isospin relation holds in the amplitudes expressed in the triangle diagrams.

The framework proposed in this work can be used to analyze other decay modes, such as  $B$  meson or heavy baryon decays. Taking the  $\bar{B} \rightarrow D\pi$  and  $\bar{B} \rightarrow \pi\pi$  decays as examples, we discuss the applications in the  $B$  meson decays in Appendix. A. One can find the conclusions in the  $D$  meson decays under the  $SU(3)_F$  symmetry can be generalized into the  $B$  meson decays under the  $SU(4)_F$  symmetry. For the heavy baryon decays, we shall leave them to the future work.

#### IV. SUMMARY

In this work, we proposed a theoretical framework to correlate the topological diagram at quark level and rescattering dynamics at hadron level. The main points are the following:

1. Both the topological diagram, quark diagram, and triangle diagram can be written in the tensor form.
2. The coefficient of each triangle diagram can be derived from the quark diagram.
3. There is one minus sign between the quark diagrams with and without a cross of quark lines. It arises from the commutator in the chiral Lagrangian.
4. The vertexes such as  $\omega\pi^+\pi^-$ ,  $\rho^0\pi^0\pi^0$  ... might appear in a triangle diagrams derived from quark diagrams. But all the contributions associated with them cancel after summing all triangle diagrams in one decay channel.
5. The completeness of the quark diagram is confirmed by the quark substructure of meson-meson scattering since there is no repeated substructure in the quark diagrams of  $T \Rightarrow T$ ,  $T \Rightarrow C$ ,  $T \Rightarrow E$ ,  $T \Rightarrow A$  and  $T \Rightarrow P$  transitions since all the twelve possible substructures are included in the quark diagrams.
6. There are no triangle diagram like long-distance contributions in the topologies  $ES$ ,  $AS$ ,  $PS$ ,  $PA$  and  $SS$  because they can be divided into several unconnected substructures by cutting off gluon propagators.
7. The triangle diagrams derived from the quark diagrams are consistent with the ones derived from the chiral Lagrangian directly.

8. Under the  $SU(3)_F$  symmetry, the rescattering contribution arisen from  $T^{SD}$  in the  $C$  diagram is  $-2$  times the ones in the  $E$  and  $P$  diagrams,  $L(C) : L(E) : L(P) = -2 : 1 : 1$ . It indicates the penguin amplitudes are the same order with the tree amplitudes, which leads to an observable CP violation in charm decay.
9. The rescattering contributions arisen from  $T^{SD}$  in the  $T$  and  $A$  diagrams are arisen from the  $SU(3)_F$  breaking effects. It could be understood in the large  $N_c$  expansion since the meson-meson scattering in the quark diagrams of  $T \Rightarrow T$  and  $T \Rightarrow A$  transitions is at order of  $1/N_c^2$  compared to  $1/N_c$  in the  $T \Rightarrow C$ ,  $T \Rightarrow E$  and  $T \Rightarrow P$  transitions. Considering the  $C^{SD}$  is one order smaller than the  $T^{SD}$ , the rescattering contributions in the  $T$  and  $A$  diagrams are smaller than  $C$ ,  $E$  and  $P$  diagrams.
10. The Isospin relations in some decay channels hold in terms of the triangle diagrams.
11. The conclusions about  $D$  meson decays under the  $SU(3)_F$  symmetry can be generalized to the  $B$  meson decays under the  $SU(4)_F$  symmetry.

### Acknowledgments

We are grateful to Hai-Yang Cheng, Fu-Sheng Yu and Cai-Ping Jia for useful discussions. This work was supported in part by the National Natural Science Foundation of China under Grants No.12105099.

### Appendix A: Application in $B$ meson decay

In this Appendix, we analyze the  $\bar{B} \rightarrow D\pi$  and  $\bar{B} \rightarrow \pi\pi$  decays as supplementary examples.

#### 1. $\bar{B} \rightarrow D\pi$ decay

The topological amplitude of  $\bar{B}^0 \rightarrow D^+\pi^-$  decay is  $T + E$ . The long-distance contributions modeled by triangle diagram include

$$L(T)_1[d, c, u, d] = \frac{1}{2}\Delta(\bar{B}^0, \pi^-, D^+, \rho^0, \pi^-, D^+) - \frac{1}{2}\Delta(\bar{B}^0, \pi^-, D^+, \omega, \pi^-, D^+), \quad (A1)$$

$$L(E)[d, d, u, c] = \frac{1}{2}\Delta(\bar{B}^0, \pi^-, D^+, \rho^0, \pi^-, D^+) + \frac{1}{2}\Delta(\bar{B}^0, \pi^-, D^+, \omega, \pi^-, D^+). \quad (A2)$$

Summing all of them, the rescattering amplitude in the  $\bar{B}^0 \rightarrow D^+\pi^-$  decay is

$$\mathcal{A}_L(\bar{B}^0 \rightarrow D^+\pi^-) = L(T)_1[d, c, u, d] + L(E)[d, d, u, c] = \Delta(\bar{B}^0, \pi^-, D^+, \rho^0, \pi^-, D^+). \quad (\text{A3})$$

The topological amplitude of  $\bar{B}^0 \rightarrow D^0\pi^0$  decay is  $-\frac{1}{\sqrt{2}}C + \frac{1}{\sqrt{2}}E$ . The rescattering contributions include

$$-\frac{1}{\sqrt{2}}L(C)_1[d, d, u, c] = \frac{1}{\sqrt{2}}\Delta(\bar{B}^0, \pi^-, D^+, \rho^-, \pi^0, D^0), \quad (\text{A4})$$

$$-\frac{1}{\sqrt{2}}L(C)_2[d, d, u, c] = \frac{1}{\sqrt{2}}\Delta(\bar{B}^0, \pi^-, D^+, D^{*-}, D^0, \pi^0), \quad (\text{A5})$$

$$\frac{1}{\sqrt{2}}L(E)[d, u, u, c] = \frac{1}{\sqrt{2}}\Delta(\bar{B}^0, \pi^-, D^+, \rho^-, \pi^0, D^0). \quad (\text{A6})$$

Summing all of them, the rescattering amplitude in the  $\bar{B}^0 \rightarrow D^0\pi^0$  decay is

$$\begin{aligned} \mathcal{A}_L(\bar{B}^0 \rightarrow D^0\pi^0) &= -\frac{1}{\sqrt{2}}L(C)_1[d, d, u, c] - \frac{1}{\sqrt{2}}L(C)_2[d, d, u, c] + \frac{1}{\sqrt{2}}L(E)[d, u, u, c] \\ &= \sqrt{2}\Delta(\bar{B}^0, \pi^-, D^+, \rho^-, \pi^0, D^0) + \frac{1}{\sqrt{2}}\Delta(\bar{B}^0, \pi^-, D^+, D^{*-}, D^0, \pi^0). \end{aligned} \quad (\text{A7})$$

The topological amplitude of  $B^- \rightarrow D^0\pi^-$  decay is  $T + C$ . The rescattering contributions include

$$L(T)_2[u, c, u, d] = -\frac{1}{2}\Delta(B^-, \pi^-, D^0, \rho^0, \pi^-, D^0) + \frac{1}{2}\Delta(B^-, \pi^-, D^0, \omega, \pi^-, D^0), \quad (\text{A8})$$

$$L(C)_1[u, d, u, c] = -\frac{1}{2}\Delta(B^-, \pi^-, D^0, \rho^0, \pi^-, D^0) - \frac{1}{2}\Delta(B^-, \pi^-, D^0, \omega, \pi^-, D^0), \quad (\text{A9})$$

$$L(C)_2[u, d, u, c] = -\Delta(B^-, \pi^-, D^0, D^{*-}, D^0, \pi^-). \quad (\text{A10})$$

Summing all of them, the rescattering amplitude in the  $D^0 \rightarrow \pi^0\pi^0$  decay is

$$\begin{aligned} \mathcal{A}_L(B^- \rightarrow D^0\pi^-) &= L(T)_2[u, c, u, d] + L(C)_1[u, d, u, c] + L(C)_2[u, d, u, c] \\ &= -\Delta(B^-, \pi^-, D^0, \rho^0, \pi^-, D^0) - \Delta(B^-, \pi^-, D^0, D^{*-}, D^0, \pi^-). \end{aligned} \quad (\text{A11})$$

Under the Isospin symmetry, we have

$$\begin{aligned} \Delta'_1 &= \Delta(\bar{B}^0, \pi^-, D^+, \rho^0, \pi^-, D^+) = \Delta(\bar{B}^0, \pi^-, D^+, \rho^-, \pi^0, D^0) = \Delta(B^-, \pi^-, D^0, \rho^0, \pi^-, D^0), \\ \Delta'_2 &= \Delta(\bar{B}^0, \pi^-, D^+, D^{*-}, D^0, \pi^0) = \Delta(B^-, \pi^-, D^0, D^{*-}, D^0, \pi^-). \end{aligned} \quad (\text{A12})$$

The decay amplitudes of  $\bar{B}^0 \rightarrow D^+\pi^-$ ,  $\bar{B}^0 \rightarrow D^0\pi^0$  and  $B^- \rightarrow D^0\pi^-$  channels can be written as

$$\begin{aligned} \mathcal{A}_L(\bar{B}^0 \rightarrow D^+\pi^-) &= \Delta'_1, \quad \mathcal{A}_L(\bar{B}^0 \rightarrow D^0\pi^0) = \sqrt{2}\Delta'_1 + \frac{1}{\sqrt{2}}\Delta'_2, \\ \mathcal{A}_L(B^- \rightarrow D^0\pi^-) &= -\Delta'_1 - \Delta'_2. \end{aligned} \quad (\text{A13})$$

One can check the Isospin relation

$$\mathcal{A}(B^- \rightarrow D^0 \pi^-) + \sqrt{2} \mathcal{A}(\bar{B}^0 \rightarrow D^0 \pi^0) = \mathcal{A}(\bar{B}^0 \rightarrow D^+ \pi^-) \quad (\text{A14})$$

is satisfied. Under the  $SU(4)_F$  symmetry, all the triangle diagrams are equivalent. The rescattering contributions of  $T$  diagrams are zero, and  $L(C) = -2 L(E)$ .

## 2. $\bar{B} \rightarrow \pi\pi$ decay

The topological amplitude of  $\bar{B}^0 \rightarrow \pi^+ \pi^-$  decay is  $\lambda_u(T + E) + \lambda_u(P + 2PA) + \lambda_c(P + 2PA)$ , in which  $\lambda_u = V_{ud}V_{ub}^*$  and  $\lambda_c = V_{cd}V_{cb}^*$ . The rescattering contributions modeled by triangle diagram include

$$\lambda_u L(T)_1[d, u, u, d] = \frac{1}{2} \lambda_u \Delta(\bar{B}^0, \pi^-, \pi^+, \rho^0, \pi^-, \pi^+) - \frac{1}{2} \lambda_u \Delta(\bar{B}^0, \pi^-, \pi^+, \omega, \pi^-, \pi^+), \quad (\text{A15})$$

$$\lambda_u L(T)_4[d, u, u, d] = \frac{1}{2} \lambda_u \Delta(\bar{B}^0, \pi^-, \pi^+, \rho^0, \pi^-, \pi^+) - \frac{1}{2} \lambda_u \Delta(\bar{B}^0, \pi^-, \pi^+, \omega, \pi^-, \pi^+), \quad (\text{A16})$$

$$\lambda_u L(E)[d, u, d, u] = \frac{1}{2} \lambda_u \Delta(\bar{B}^0, \pi^-, \pi^+, \rho^0, \pi^-, \pi^+) + \frac{1}{2} \lambda_u \Delta(\bar{B}^0, \pi^-, \pi^+, \omega, \pi^-, \pi^+), \quad (\text{A17})$$

$$\lambda_u L(P)[d, u, d, u] = \frac{1}{2} \lambda_u \Delta(\bar{B}^0, \pi^-, \pi^+, \rho^0, \pi^-, \pi^+) + \frac{1}{2} \lambda_u \Delta(\bar{B}^0, \pi^-, \pi^+, \omega, \pi^-, \pi^+), \quad (\text{A18})$$

$$\lambda_c L(P)[d, u, d, c] = \lambda_c \Delta(\bar{B}^0, D^-, D^+, \bar{D}^{*0}, \pi^-, \pi^+). \quad (\text{A19})$$

Summing all of them, the rescattering amplitude in the  $\bar{B}^0 \rightarrow \pi^+ \pi^-$  decay is

$$\begin{aligned} \mathcal{A}_L(\bar{B}^0 \rightarrow \pi^+ \pi^-) &= \lambda_u(L(T)_1[d, u, u, d] + L(T)_4[d, u, u, d] + L(E)[d, u, d, u] \\ &\quad + L(P)[d, u, d, u]) + \lambda_c L(P)[d, u, d, c] \\ &= 2\lambda_u \Delta(\bar{B}^0, \pi^-, \pi^+, \rho^0, \pi^-, \pi^+) + \lambda_c \Delta(\bar{B}^0, D^-, D^+, \bar{D}^{*0}, \pi^-, \pi^+). \end{aligned} \quad (\text{A20})$$

The topological amplitude of  $\bar{B}^0 \rightarrow \pi^0 \pi^0$  decay is  $\frac{1}{\sqrt{2}} \lambda_u(E - C) + \frac{1}{\sqrt{2}} \lambda_u(P + 2PA) + \frac{1}{\sqrt{2}} \lambda_c(P + 2PA)$ .

The rescattering contributions include

$$\frac{1}{\sqrt{2}} \lambda_u L(E)[d, u, u, u] = \frac{1}{\sqrt{2}} \lambda_u \Delta(\bar{B}^0, \pi^-, \pi^+, \rho^-, \pi^0, \pi^0), \quad (\text{A21})$$

$$-\frac{1}{\sqrt{2}} \lambda_u L(C)_1[d, d, u, u] = \frac{1}{\sqrt{2}} \lambda_u \Delta(\bar{B}^0, \pi^-, \pi^+, \rho^-, \pi^0, \pi^0), \quad (\text{A22})$$

$$-\frac{1}{\sqrt{2}} \lambda_u L(C)_2[d, d, u, u] = \frac{1}{\sqrt{2}} \lambda_u \Delta(\bar{B}^0, \pi^-, \pi^+, \rho^-, \pi^0, \pi^0), \quad (\text{A23})$$

$$\frac{1}{\sqrt{2}} \lambda_u L(P)[d, d, d, u] = \frac{1}{\sqrt{2}} \lambda_u \Delta(\bar{B}^0, \pi^-, \pi^+, \rho^-, \pi^0, \pi^0), \quad (\text{A24})$$

$$\frac{1}{\sqrt{2}} \lambda_c L(P)[d, d, d, c] = \frac{1}{\sqrt{2}} \lambda_c \Delta(\bar{B}^0, D^-, D^+, D^{*-}, \pi^0, \pi^0). \quad (\text{A25})$$



Summing all of them, the rescattering amplitude in the  $\bar{B}^0 \rightarrow \pi^0 \pi^0$  decay is

$$\begin{aligned}\mathcal{A}_L(\bar{B}^0 \rightarrow \pi^0 \pi^0) &= \frac{1}{\sqrt{2}} \lambda_d (L(E)[d, u, u, u] - L(C)_1[d, d, u, u] - L(C)_2[d, d, u, u] \\ &\quad + L(P)[d, d, d, u]) + \frac{1}{\sqrt{2}} \lambda_c L(P)[d, d, d, c] \\ &= 2\sqrt{2} \lambda_u \Delta(\bar{B}^0, \pi^-, \pi^+, \rho^-, \pi^0, \pi^0) + \frac{1}{\sqrt{2}} \lambda_c \Delta(\bar{B}^0, D^-, D^+, D^{*-}, \pi^0, \pi^0).\end{aligned}\quad (\text{A26})$$

The topological amplitude of  $B^- \rightarrow \pi^- \pi^0$  decay is  $\frac{1}{\sqrt{2}} \lambda_u (T + C)$ . The rescattering contributions include

$$\begin{aligned}\frac{1}{\sqrt{2}} \lambda_u L(T)_2[u, u, d, u] &= -\frac{1}{4\sqrt{2}} \lambda_u \Delta(B^-, \pi^-, \pi^0, \rho^0, \pi^-, \pi^0) - \frac{1}{12\sqrt{2}} \lambda_u \Delta(B^-, \pi^-, \eta_8, \rho^0, \pi^-, \pi^0) \\ &\quad - \frac{1}{6\sqrt{2}} \lambda_u \Delta(B^-, \pi^-, \eta_1, \rho^0, \pi^-, \pi^0) + \frac{1}{4\sqrt{2}} \lambda_u \Delta(B^-, \pi^-, \pi^0, \omega, \pi^-, \pi^0) \\ &\quad + \frac{1}{12\sqrt{2}} \lambda_u \Delta(B^-, \pi^-, \eta_8, \omega, \pi^-, \pi^0) + \frac{1}{6\sqrt{2}} \lambda_u \Delta(B^-, \pi^-, \eta_1, \omega, \pi^-, \pi^0),\end{aligned}\quad (\text{A27})$$

$$\begin{aligned}\frac{1}{\sqrt{2}} \lambda_u L(T)_4[u, u, d, u] &= \frac{1}{4\sqrt{2}} \lambda_u \Delta(B^-, \pi^-, \pi^0, \rho^0, \pi^-, \pi^0) + \frac{1}{12\sqrt{2}} \lambda_u \Delta(B^-, \pi^-, \eta_8, \rho^0, \pi^-, \pi^0) \\ &\quad + \frac{1}{6\sqrt{2}} \lambda_u \Delta(B^-, \pi^-, \eta_1, \rho^0, \pi^-, \pi^0) - \frac{1}{4\sqrt{2}} \lambda_u \Delta(B^-, \pi^-, \pi^0, \omega, \pi^-, \pi^0) \\ &\quad - \frac{1}{12\sqrt{2}} \lambda_u \Delta(B^-, \pi^-, \eta_8, \omega, \pi^-, \pi^0) - \frac{1}{6\sqrt{2}} \lambda_u \Delta(B^-, \pi^-, \eta_1, \omega, \pi^-, \pi^0),\end{aligned}\quad (\text{A28})$$

$$\begin{aligned}\frac{1}{\sqrt{2}} \lambda_u L(C)_1[u, d, u, u] &= -\frac{1}{4\sqrt{2}} \lambda_u \Delta(B^-, \pi^-, \pi^0, \rho^0, \pi^-, \pi^0) - \frac{1}{12\sqrt{2}} \lambda_u \Delta(B^-, \pi^-, \eta_8, \rho^0, \pi^-, \pi^0) \\ &\quad - \frac{1}{6\sqrt{2}} \lambda_u \Delta(B^-, \pi^-, \eta_1, \rho^0, \pi^-, \pi^0) - \frac{1}{4\sqrt{2}} \lambda_u \Delta(B^-, \pi^-, \pi^0, \omega, \pi^-, \pi^0) \\ &\quad - \frac{1}{12\sqrt{2}} \lambda_u \Delta(B^-, \pi^-, \eta_8, \omega, \pi^-, \pi^0) - \frac{1}{6\sqrt{2}} \lambda_u \Delta(B^-, \pi^-, \eta_1, \omega, \pi^-, \pi^0),\end{aligned}\quad (\text{A29})$$

$$\begin{aligned}\frac{1}{\sqrt{2}} \lambda_u L(C)_2[u, d, u, u] &= -\frac{1}{2\sqrt{2}} \lambda_u \Delta(B^-, \pi^-, \pi^0, \rho^-, \pi^0, \pi^-) - \frac{1}{6\sqrt{2}} \lambda_u \Delta(B^-, \pi^-, \eta_8, \rho^-, \pi^0, \pi^-) \\ &\quad - \frac{1}{3\sqrt{2}} \lambda_u \Delta(B^-, \pi^-, \eta_1, \rho^-, \pi^0, \pi^-),\end{aligned}\quad (\text{A30})$$

$$\begin{aligned}
-\frac{1}{\sqrt{2}}\lambda_u L(A)_1[u, u, d, d] &= -\frac{1}{4\sqrt{2}}\lambda_u \Delta(B^-, \pi^-, \pi^0, \rho^0, \pi^-, \pi^0) + \frac{1}{12\sqrt{2}}\lambda_u \Delta(B^-, \pi^-, \eta_8, \rho^0, \pi^-, \pi^0) \\
&+ \frac{1}{6\sqrt{2}}\lambda_u \Delta(B^-, \pi^-, \eta_1, \rho^0, \pi^-, \pi^0) - \frac{1}{4\sqrt{2}}\lambda_u \Delta(B^-, \pi^-, \pi^0, \omega, \pi^-, \pi^0) \\
&+ \frac{1}{12\sqrt{2}}\lambda_u \Delta(B^-, \pi^-, \eta_8, \omega, \pi^-, \pi^0) + \frac{1}{6\sqrt{2}}\lambda_u \Delta(B^-, \pi^-, \eta_1, \rho^0, \pi^-, \pi^0),
\end{aligned} \tag{A31}$$

$$\begin{aligned}
-\frac{1}{\sqrt{2}}\lambda_u L(A)_2[u, u, d, d] &= -\frac{1}{2\sqrt{2}}\lambda_u \Delta(B^-, \pi^-, \pi^0, \rho^-, \pi^0, \pi^-) + \frac{1}{6\sqrt{2}}\lambda_u \Delta(B^-, \pi^-, \eta_8, \rho^-, \pi^0, \pi^-) \\
&+ \frac{1}{3\sqrt{2}}\lambda_u \Delta(B^-, \pi^-, \eta_1, \rho^-, \pi^0, \pi^-),
\end{aligned} \tag{A32}$$

$$\begin{aligned}
-\frac{1}{\sqrt{2}}\lambda_u L(A)_3[u, u, u, d] &= +\frac{1}{4\sqrt{2}}\lambda_u \Delta(B^-, \pi^-, \pi^0, \rho^0, \pi^-, \pi^0) - \frac{1}{12\sqrt{2}}\lambda_u \Delta(B^-, \pi^-, \eta_8, \rho^0, \pi^-, \pi^0) \\
&- \frac{1}{6\sqrt{2}}\lambda_u \Delta(B^-, \pi^-, \eta_1, \rho^0, \pi^-, \pi^0) + \frac{1}{4\sqrt{2}}\lambda_u \Delta(B^-, \pi^-, \pi^0, \omega, \pi^-, \pi^0) \\
&- \frac{1}{12\sqrt{2}}\lambda_u \Delta(B^-, \pi^-, \eta_8, \omega, \pi^-, \pi^0) - \frac{1}{6\sqrt{2}}\lambda_u \Delta(B^-, \pi^-, \eta_1, \rho^0, \pi^-, \pi^0),
\end{aligned} \tag{A33}$$

$$\begin{aligned}
\frac{1}{\sqrt{2}}\lambda_u L(A)_3[u, u, d, d] &= -\frac{1}{2\sqrt{2}}\lambda_u \Delta(B^-, \pi^-, \pi^0, \rho^-, \pi^0, \pi^-) + \frac{1}{6\sqrt{2}}\lambda_u \Delta(B^-, \pi^-, \eta_8, \rho^-, \pi^0, \pi^-) \\
&+ \frac{1}{3\sqrt{2}}\lambda_u \Delta(B^-, \pi^-, \eta_1, \rho^-, \pi^0, \pi^-),
\end{aligned} \tag{A34}$$

$$\begin{aligned}
\frac{1}{\sqrt{2}}\lambda_u L(P)[u, u, d, u] &= \frac{1}{4\sqrt{2}}\lambda_u \Delta(B^-, \pi^-, \pi^0, \rho^0, \pi^-, \pi^0) + \frac{1}{12\sqrt{2}}\lambda_u \Delta(B^-, \pi^-, \eta_8, \rho^0, \pi^-, \pi^0) \\
&+ \frac{1}{6\sqrt{2}}\lambda_u \Delta(B^-, \pi^-, \eta_1, \rho^0, \pi^-, \pi^0) + \frac{1}{4\sqrt{2}}\lambda_u \Delta(B^-, \pi^-, \pi^0, \omega, \pi^-, \pi^0) \\
&+ \frac{1}{12\sqrt{2}}\lambda_u \Delta(B^-, \pi^-, \eta_8, \omega, \pi^-, \pi^0) + \frac{1}{6\sqrt{2}}\lambda_u \Delta(B^-, \pi^-, \eta_1, \rho^0, \pi^-, \pi^0),
\end{aligned} \tag{A35}$$

$$\begin{aligned}
-\frac{1}{\sqrt{2}}\lambda_u L(P)[u, d, d, u] &= -\frac{1}{2\sqrt{2}}\lambda_u \Delta(B^-, \pi^-, \pi^0, \rho^-, \pi^0, \pi^-) - \frac{1}{6\sqrt{2}}\lambda_u \Delta(B^-, \pi^-, \eta_8, \rho^-, \pi^0, \pi^-) \\
&- \frac{1}{3\sqrt{2}}\lambda_u \Delta(B^-, \pi^-, \eta_1, \rho^-, \pi^0, \pi^-),
\end{aligned} \tag{A36}$$

$$\frac{1}{\sqrt{2}}\lambda_c L(P)[u, u, d, c] = \frac{1}{\sqrt{2}}\lambda_c \Delta(B^-, D^-, D^0, \bar{D}^{*0}, \pi^-, \pi^0), \tag{A37}$$

$$-\frac{1}{\sqrt{2}}\lambda_c L(P)[u, d, d, c] = -\frac{1}{\sqrt{2}}\lambda_c \Delta(B^-, D^-, D^0, D^{*-}, \pi^0, \pi^-). \tag{A38}$$

Summing all quark diagrams, the rescattering amplitude in the  $B^- \rightarrow \pi^- \pi^0$  decay is

$$\begin{aligned}
\mathcal{A}_L(B^- \rightarrow \pi^- \pi^0) &= \frac{1}{\sqrt{2}} \lambda_u (L(T)_2[u, u, d, u] + L(T)_4[u, u, d, u] + L(C)_1[u, d, u, u] \\
&\quad + L(C)_2[u, d, u, u] - L(A)_1[u, u, d, d] - L(A)_2[u, u, d, d] \\
&\quad - L(A)_3[u, u, u, d] + L(A)_3[u, u, d, d] + L(P)[u, u, d, u] \\
&\quad - L(P)[u, d, d, u]) + \frac{1}{\sqrt{2}} \lambda_c (L(P)[u, u, d, c] - L(P)[u, d, d, c]) \\
&= -\sqrt{2} \lambda_u \Delta(B^-, \pi^-, \pi^0, \rho^-, \pi^0, \pi^-) + \frac{1}{\sqrt{2}} \lambda_c (\Delta(B^-, D^-, D^0, \bar{D}^{*0}, \pi^-, \pi^0) \\
&\quad - \Delta(B^-, D^-, D^0, D^{*-}, \pi^0, \pi^-)). \tag{A39}
\end{aligned}$$

Under the Isospin symmetry, we have

$$\begin{aligned}
\Delta'_3 &= \Delta(\bar{B}^0, \pi^-, \pi^+, \rho^0, \pi^-, \pi^+) = \Delta(\bar{B}^0, \pi^-, \pi^+, \rho^-, \pi^0, \pi^0) = \Delta(B^-, \pi^-, \pi^0, \rho^-, \pi^0, \pi^-), \\
\Delta'_4 &= \Delta(\bar{B}^0, D^-, D^+, \bar{D}^{*0}, \pi^-, \pi^+) = \Delta(\bar{B}^0, D^-, D^+, D^{*-}, \pi^0, \pi^0) \\
&= \Delta(B^-, D^-, D^0, \bar{D}^{*0}, \pi^-, \pi^0) = \Delta(B^-, D^-, D^0, D^{*-}, \pi^0, \pi^-). \tag{A40}
\end{aligned}$$

The decay amplitudes of  $\bar{B}^0 \rightarrow \pi^+ \pi^-$ ,  $\bar{B}^0 \rightarrow \pi^0 \pi^0$  and  $B^- \rightarrow \pi^- \pi^0$  channels can be written as

$$\begin{aligned}
\mathcal{A}_L(\bar{B}^0 \rightarrow \pi^+ \pi^-) &= 2\lambda_u \Delta'_3 + \lambda_c \Delta'_4, \quad \mathcal{A}_L(\bar{B}^0 \rightarrow \pi^0 \pi^0) = 2\sqrt{2} \lambda_u \Delta'_3 + \frac{1}{\sqrt{2}} \lambda_c \Delta'_4, \\
\mathcal{A}_L(B^- \rightarrow \pi^- \pi^0) &= -\sqrt{2} \lambda_u \Delta'_3. \tag{A41}
\end{aligned}$$

One can check the Isospin relation is maintained

$$\mathcal{A}(\bar{B}^0 \rightarrow \pi^+ \pi^-) = \sqrt{2} \mathcal{A}(\bar{B}^0 \rightarrow \pi^0 \pi^0) + \sqrt{2} \mathcal{A}(B^- \rightarrow \pi^- \pi^0). \tag{A42}$$

- 
- [1] P. A. Zyla *et al.* [Particle Data Group], PTEP **2020**, no.8, 083C01 (2020).
  - [2] M. Beneke, G. Buchalla, M. Neubert and C. T. Sachrajda, Phys. Rev. Lett. **83**, 1914 (1999) [hep-ph/9905312].
  - [3] M. Beneke, G. Buchalla, M. Neubert and C. T. Sachrajda, Nucl. Phys. B **591**, 313 (2000) [hep-ph/0006124].
  - [4] M. Beneke, G. Buchalla, M. Neubert and C. T. Sachrajda, Nucl. Phys. B **606**, 245 (2001) [hep-ph/0104110].
  - [5] M. Beneke and M. Neubert, Nucl. Phys. B **675**, 333 (2003) [hep-ph/0308039].
  - [6] Y. Y. Keum, H. n. Li and A. I. Sanda, Phys. Lett. B **504**, 6 (2001) [hep-ph/0004004].
  - [7] Y. Y. Keum, H. N. Li and A. I. Sanda, Phys. Rev. D **63**, 054008 (2001) [hep-ph/0004173].

- [8] C. D. Lu, K. Ukai and M. Z. Yang, Phys. Rev. D **63**, 074009 (2001) [hep-ph/0004213].
- [9] C. D. Lu and M. Z. Yang, Eur. Phys. J. C **23**, 275 (2002) [hep-ph/0011238].
- [10] C. W. Bauer, D. Pirjol and I. W. Stewart, Phys. Rev. Lett. **87**, 201806 (2001) [hep-ph/0107002].
- [11] C. W. Bauer, D. Pirjol and I. W. Stewart, Phys. Rev. D **65**, 054022 (2002) [hep-ph/0109045].
- [12] T. G. Rizzo and L. L. C. Wang, BNL-27950.
- [13] D. Zeppenfeld, Z. Phys. C **8**, 77 (1981).
- [14] L. L. Chau, Phys. Rept. **95**, 1 (1983).
- [15] L. L. Chau and H. Y. Cheng, Phys. Rev. Lett. **56**, 1655 (1986).
- [16] L. L. Chau and H. Y. Cheng, Phys. Rev. D **36**, 137 (1987) Addendum: [Phys. Rev. D **39**, 2788 (1989)].
- [17] H. Y. Cheng and C. W. Chiang, Phys. Rev. D **81**, 074021 (2010) [arXiv:1001.0987 [hep-ph]].
- [18] H. Y. Cheng and C. W. Chiang, Phys. Rev. D **85**, 034036 (2012) Erratum: [Phys. Rev. D **85**, 079903 (2012)] [arXiv:1201.0785 [hep-ph]].
- [19] H. Y. Cheng and C. W. Chiang, Phys. Rev. D **86**, 014014 (2012) [arXiv:1205.0580 [hep-ph]].
- [20] H. Y. Cheng, C. W. Chiang and A. L. Kuo, Phys. Rev. D **91**, no.1, 014011 (2015) [arXiv:1409.5026 [hep-ph]].
- [21] H. Y. Cheng, C. W. Chiang and A. L. Kuo, Phys. Rev. D **93**, no.11, 114010 (2016) [arXiv:1604.03761 [hep-ph]].
- [22] S. Müller, U. Nierste and S. Schacht, Phys. Rev. D **92**, no.1, 014004 (2015) [arXiv:1503.06759 [hep-ph]].
- [23] H. n. Li, C. D. Lu and F. S. Yu, Phys. Rev. D **86**, 036012 (2012) [arXiv:1203.3120 [hep-ph]].
- [24] Q. Qin, H. n. Li, C. D. Lü and F. S. Yu, Phys. Rev. D **89**, no.5, 054006 (2014) [arXiv:1305.7021 [hep-ph]].
- [25] D. Wang, F. S. Yu, P. F. Guo and H. Y. Jiang, Phys. Rev. D **95**, no.7, 073007 (2017) [arXiv:1701.07173 [hep-ph]].
- [26] H. Y. Jiang, F. S. Yu, Q. Qin, H. n. Li and C. D. Lü, Chin. Phys. C **42**, no.6, 063101 (2018) [arXiv:1705.07335 [hep-ph]].
- [27] F. S. Yu, D. Wang and H. n. Li, Phys. Rev. Lett. **119**, no.18, 181802 (2017) [arXiv:1707.09297 [hep-ph]].
- [28] S. H. Zhou, Y. B. Wei, Q. Qin, Y. Li, F. S. Yu and C. D. Lu, Phys. Rev. D **92**, no.9, 094016 (2015) [arXiv:1509.04060 [hep-ph]].
- [29] S. H. Zhou, Q. A. Zhang, W. R. Lyu and C. D. Lü, Eur. Phys. J. C **77**, no.2, 125 (2017) [arXiv:1608.02819 [hep-ph]].
- [30] C. Wang, Q. A. Zhang, Y. Li and C. D. Lu, Eur. Phys. J. C **77**, no.5, 333 (2017) [arXiv:1701.01300 [hep-ph]].
- [31] S. H. Zhou, R. H. Li, Z. Y. Wei and C. D. Lu, [arXiv:2107.11079 [hep-ph]].
- [32] X. G. He and W. Wang, Chin. Phys. C **42**, 103108 (2018) [arXiv:1803.04227 [hep-ph]].
- [33] X. G. He, Y. J. Shi and W. Wang, Eur. Phys. J. C **80**, no.5, 359 (2020) [arXiv:1811.03480 [hep-ph]].
- [34] D. Wang, C. P. Jia and F. S. Yu, JHEP **09**, 126 (2021) [arXiv:2001.09460 [hep-ph]].
- [35] X. Q. Li and B. S. Zou, Phys. Lett. B **399**, 297-302 (1997) [arXiv:hep-ph/9611223 [hep-ph]].

- [36] Y. S. Dai, D. S. Du, X. Q. Li, Z. T. Wei and B. S. Zou, Phys. Rev. D **60**, 014014 (1999) [arXiv:hep-ph/9903204 [hep-ph]].
- [37] J. W. Li, M. Z. Yang and D. S. Du, HEPNP **27**, 665-672 (2003) [arXiv:hep-ph/0206154 [hep-ph]].
- [38] M. Ablikim, D. S. Du and M. Z. Yang, Phys. Lett. B **536**, 34-42 (2002) [arXiv:hep-ph/0201168 [hep-ph]].
- [39] H. Y. Cheng, Eur. Phys. J. C **26**, 551-565 (2003) [arXiv:hep-ph/0202254 [hep-ph]].
- [40] H. Y. Cheng, C. K. Chua and A. Soni, Phys. Rev. D **71**, 014030 (2005) [arXiv:hep-ph/0409317 [hep-ph]].
- [41] C. D. Lu, Y. L. Shen and W. Wang, Phys. Rev. D **73**, 034005 (2006) [arXiv:hep-ph/0511255 [hep-ph]].
- [42] M. P. Locher, Y. Lu and B. S. Zou, Z. Phys. A **347**, 281-284 (1994) [arXiv:nucl-th/9311021 [nucl-th]].
- [43] S. L. Chen, X. H. Guo, X. Q. Li and G. L. Wang, Commun. Theor. Phys. **40**, 563-572 (2003) [arXiv:hep-ph/0208006 [hep-ph]].
- [44] J. J. Han, R. X. Zhang, H. Y. Jiang, Z. J. Xiao and F. S. Yu, Eur. Phys. J. C **81**, no.6, 539 (2021) [arXiv:2102.00961 [hep-ph]].
- [45] F. S. Yu, H. Y. Jiang, R. H. Li, C. D. Lü, W. Wang and Z. X. Zhao, Chin. Phys. C **42**, no.5, 051001 (2018) [arXiv:1703.09086 [hep-ph]].
- [46] R. Aaij *et al.* [LHCb], Phys. Rev. Lett. **119**, no.11, 112001 (2017) [arXiv:1707.01621 [hep-ex]].
- [47] L. J. Jiang, B. He and R. H. Li, Eur. Phys. J. C **78**, no.11, 961 (2018) [arXiv:1810.00541 [hep-ph]].
- [48] J. J. Han, H. Y. Jiang, W. Liu, Z. J. Xiao and F. S. Yu, Chin. Phys. C **45**, no.5, 053105 (2021) [arXiv:2101.12019 [hep-ph]].
- [49] Morse P, HermanFeshbach; “Methods of Theoretical Physics [J],” American Journal of Physics, 22(6):410-413, (1954).
- [50] S. Okubo, Phys. Lett. 5, 165 (1963).
- [51] G. Zweig, CERN Report No.8419/TH412 (1964).
- [52] J. Iizuka, Prog. Theor. Phys. Suppl. 37, 21 (1966).
- [53] R. Aaij *et al.* [LHCb Collaboration], Phys. Rev. Lett. **122**, no. 21, 211803 (2019) [arXiv:1903.08726 [hep-ex]].
- [54] Y. Grossman and S. Schacht, JHEP **1907**, 020 (2019) [arXiv:1903.10952 [hep-ph]].